ivia
Institut Valencià
d'Investigacions Agràries

# Blade pitch and air-outlet width effects on the airflow generated by an airblast sprayer with wireless remote-controlled axial fan

Ramón Salcedo[1,2,3], Alberto Fonte[1], Marco Grella[4], Cruz Garcerá[1], Patricia Chueca[1*]

[1] Centro de Agroingeniería, Instituto Valenciano de Investigaciones Agrarias (IVIA); CV-315, km 10.7; 46113 Moncada, Valencia, Spain.

[2] Department of Food Agricultural and Biological Engineering (FABE), The Ohio State University, Columbus, Ohio, United States.

[3] Application Technology Research Unit (ATRU), Agricultural Research Service of the United States Department of Agriculture (USDA-ARS), Wooster, Ohio, United States.

[4] Department of Agricultural, Forest and Food Sciences (DiSAFA), University of Turin (UNITO), Largo Paolo Braccini, 2, 10095 Grugliasco (TO), Italy.

[*]**Corresponding Author:** Patricia Chueca Adell. Mail: chueca_pat@gva.es; Tel: +34 96 342 40 00; Fax: +34 96 342 40 01

**Open Researcher and Contributor ID (ORCID) of the authors:** R. Salcedo: 0000-0003-4798-1443; A. Fonte: 0000-0003-1757-3713; M. Grella: 0000-0002-5932-8495; C. Garcerá: 0000-0001-5810-7538; P. Chueca: 0000-0001-9333-8083

21  **Abstract**

22  The airblast sprayers are equipped with a fan generating an air stream that helps the
23  sprayed droplets to reach out and penetrate the tree canopy. Recently an automatic air
24  regulation system has been developed and integrated in an airblast sprayer equipped
25  with a conventional axial fan (900 mm diameter). This system, thanks to a wireless
26  connection between a dedicated tablet and sprayers actuators, allows to remotely control
27  the blade pitch and the air-outlet section, varying the characteristics of airflow generated
28  by the fan. Therefore, the present work aims to characterize the different air streams
29  derived from the combination of two fan outlet section widths (110 and 150 mm) and
30  three blade pitches (20°, 25° and 30°). For each combination, the three components of
31  air velocity (m s$^{-1}$) were measured, taking as reference the plane following the
32  theoretical trajectory of the main current leaving the fan. In this plane, velocities were
33  measured at 1.0, 3.0, 5.0 and 10.0 m from the outlet section on both sides of the sprayer.
34  At each distance, the velocities from 0.25 to 4.00 m in height were recorded. This same
35  procedure was repeated in two planes parallel to the reference plane, 0.30 m behind and
36  after respectively. Additionally, the velocities in the fan outlet section were also
37  measured to obtain the airflow rate. In general, the outlet section and the blade pitch had
38  a significant effect on the velocity components. An outlet section of 110 mm meant a
39  smaller airflow rate and a higher initial velocity, while with 150 mm the airflow rate
40  reduced and the initial velocity decreased. Velocities could be bigger by enhancing the
41  blade pitch. The turbulence intensity was similar at 1.0 m distance in all cases.

42  **Keywords:** pesticide application; air currents; velocity vectors; turbulence intensity; 3D
43  sonic anemometer.

44

## 1. Introduction

Pesticide spray applications from the ground in three dimensional (3D) crops are usually performed vertically (sidewards), with a flow penetrating different layers of vegetation to reach the inner part. It is necessary to lead the spray into the target crop and move the leaves to facilitate the spray deposition, for this reason, the sprayers are usually air assisted. They can be equipped with different types of fans, which could be differentiated into three main groups, according to the engineering design, namely axial, centrifugal and tangential ( wiechowski et al., 2004; Dekeyser et al., 2011). In general, the centrifugal fans are characterized by low volume and very high velocity. They are normally used when the air discharge system is featured by individual spouts ( wiechowski et al., 2004; Doruchowski et al., 2011; Grella et al., 2019) coupled with hydraulic atomization, when the sprayed droplets have to travel long distances to reach the target, i.e. very big plantations, as poplar (Grella et al., 2017a), or with pneumatic atomization, because in all these cases very high velocity is needed (Balsari et al., 2019; Grella et al., 2020a). Tangential fans are well known to present low values for both parameters, air volume and velocity. For this reason, they could reduce the spray drift during treatments, but they are expensive and show very limited operational flexibility (Cross et al., 2003; Di Prinzio et al., 2004).

Axial fans produce radial air currents characterized by high volume and low velocity, which penetrate the canopies more effectively than lower volume and/or higher velocity currents (Randall, 1971; Triloff, 2015, 2016), and for these reasons are the most usual in sprayers for application in 3D crops, because of the great volume and low velocity. Airflow rate capacity of sprayers with axial fans ranges between 10,000 and 100,000 $m^3$ $h^{-1}$ depending on the fan diameter, number, shape, and pitch of blades, the air-outlet width, and the rotating speed (Whitney et al., 1986; Walklate et al., 1996; Cross et al., 2003; Pascuzzi et al., 2017; Van de Zande et al., 2017; Marucco et al., 2019; Bahlol et al., 2019; Failla et al., 2020a, 2020b; Wenneker et al., 2020). The right selection of the fan dimensions and its technical specifications have to be accurately done by the sprayersø manufacturers considering the target crop. For this reason, there are specific sprayers for vineyards, fruit orchards, citrus, olives, and other 3D crops on the market (Zhu et al., 2006; Pergher et al., 2013; Salyani et al., 2013; Grella et al., 2017b; Kasner

76    et al., 2020).

77    Fan airflow characteristics together with forward speed and their interactions have a
78    strong influence on both canopy deposition and off-target losses (Walklate et al., 1996;
79    Pergher, 2006), which many authors mainly attribute to the design of the sprayer air
80    discharge system (Dekeyser et al., 2014; Triloff, 2015; Grella et al., 2020b).

81    To ensure the spray coverage at the top of the tree, the axial fan is normally set in the
82    way that the spray overshoots the canopy top and this causes a significant part of the
83    spray volume to be delivered into the open atmosphere above the crop (Delele et al.,
84    2007; Llorens at al., 2016) being easily swept along by natural wind and resulting in
85    spray drift at further distances from the target area (Gil and Sinfort; 2005; Felsot et al.,
86    2011). The reduction of spray drift represents a major challenge when applying
87    agrochemicals as non-target receptors can be exposed to pesticide adverse effects (Jong
88    et al., 2008; Otto et al., 2009; Garcerá et al., 2017b; Butler-Ellis et al., 2017; Ochoa and
89    Maestroni, 2018). It derives that the spray drift containment is an essential aspect to
90    take into account during the design and set up of axial fan-assisted sprayers (Otto et al.,
91    2015; Fornasiero et al., 2017).

92    The right adjustment of air jet (adjustment of fan airflow rate, velocity and, if possible,
93    direction), depending on the canopy size, leaf density and row distance, would result in
94    a reduction of spray drift and ground losses, and an increase of leaf deposition, that is,
95    an improvement of application efficiency, and thus this adjustment plays a key role in
96    the efficacy and the environmental sustainability of pesticide applications (Fox et al.,
97    1992; Vereecke et al., 2000; Svensson et al., 2002, 2003; Cross et al., 2003; Balsari et
98    al., 2008; Pai et al., 2009; Salyani et al., 2013; Miranda-Fuentes et al., 2015; Salcedo et
99    al., 2015; Wennecker et al., 2020).

100   While different methodologies have been already established to determine the optimal
101   spray application rate depending on the canopy characteristics (Rüegg et al., 2006;
102   Llorens et al., 2010; Doruchowsky et al., 2011; Gil et al., 2011; Garcerá et al. 2017a),
103   very few data exist concerning the best relationship between airflow characteristics and
104   canopy architecture to achieve the best foliar deposition, minimizing at the same time
105   off-target losses. Recommendation manuals (TOPPS, 2014), informatics tools

106  (Doruchowski et al., 2013, 2014), and devices (Gil et al., 2015; Bahlol et al., 2020) that
107  allow to roughly adjust the airflow characteristics to the target had been developed.
108  However, such tools cannot be easily accessed by the end-users, and in most cases, the
109  airflow adjustment is totally left to the operator's skills and experience. On the other
110  hand, the current provision of airflow adjustment on many commercial sprayers is
111  generally inadequate to obtain optimal spray distribution patterns across the broad range
112  of canopy structures that exists in many farms (Cross et al., 2003; Marucco et al., 2020)
113  because in most cases it is only possible to select between low and high fan speed.
114  Furthermore, the technical manuals of the sprayers do not provide detailed information
115  on the characteristics of the airflow generated by the fan (García-Ramos et al., 2012)
116  and how to adjust the airflow to the target characteristics.

117  In order to improve the airflow penetration into the canopy and to reduce the off-target
118  losses, a few sprayers with adjustable fan settings able to vary continuously and in real
119  time the airflow characteristics according to the needs have been developed. These
120  sprayers are either equipped with several axial fans mounted in different positions on
121  the sprayer or can change the width of the air outlet channel and/or the blades pitch, etc.
122  (García-Ramos et al., 2009, 2012; Endalew et al., 2010a, 2010b; Holownicki et al.,
123  2017). In this context, the detailed physical description of the fan airflow behavior and
124  the effect of the different parameters are important to understand the whole
125  phenomenon. It would help the manufacturers to improve the design of the sprayersøfan
126  to make it possible to adjust its settings to the airflow requirements in a specific
127  application.

128  The objective of this work was to study the behavior of the airflow generated by an
129  axial fan sprayer with an electronic control-system capable of modifying the air outlet
130  width and the fan-blades pitch remotely. Specifically, the characteristics of different
131  airflows, resulting from a combination of these two variable parameters, were
132  investigated at different distances and heights from the fan.

## 2. Material and methods

The behavior of the airflow generated by the axial fan sprayer and the influence of blades pitch and air outlet width on the air currents was studied in static conditions, this is, with no motion of the sprayer and without considering crop interaction. Considering the relationship between static and dynamic measurements the static analysis still remains a useful tool to predict the sprayer performance in dynamic conditions (De Moor et al., 2002; Delele et al., 2005).

### 2.1. Experimental site

The trials were conducted indoor at Instituto Valenciano de Investigaciones Agrarias facilities (Moncada, Valencia, Spain; 39°35'18.7"N 0°23'43.4"W), in order to minimize interferences among sprayer fan airflow and environmental wind currents. The warehouse were 9.8 m width and 43.5 m long with a gable roof with 6.0 m high in the top and 4.5 m high in the bottom. No noticeable obstacles were present inside the building. Surfaces of the walls and ground were smooth, so the friction effect generated and its influence were considered negligible at the measuring positions as other authors (Da Silva et al., 2006; Dekeyser et al., 2013; Van de Zande et al., 2017).

### 2.2. Sprayer features

A conventional trailed axial fan sprayer John Deere mod. R120 (John Deere, Moline, IL, United States) with a 2,000 L polyethylene tank (Fig. 1a) connected to a tractor New Holland mod. TN95NA (CNH Industrial, Torino, Italy) was employed. In particular, it was equipped with the axial fan mod. FUTUR remotely controlled by the H3O® system developed by Pulverizadores Fede (Valencia, Spain) (Garcerá et al., 2018, Berger et al., 2019). Substantially, the H3O® system allowed to monitor and modify the spray application parameters according to the canopy size and working conditions.

158



159

**Fig. 1.** Axial fan sprayer used for the experiment: general view (a) and air outlet channels detailed (b): channels A (variable width), B and C (fixed width). The dotted lines indicate how the half-length (H-L) of channels A, B and C was measured.

163

The sprayer was sized for spray applications in high-density tree crops such as citrus. Therefore the fan's diameter was 900 mm with eight fiberglass-reinforced nylon blades rotating anticlockwise (viewing the fan from the rear of the sprayer) and two possible fan gear speed, namely low and high. In order to reduce the airflow asymmetry between sprayer sides, due to the fan rotation direction, a deflector in the air inlet was provided; it derives twelve vanes curved back. Concurrently, the fan outlet section was composed by three vertical channels (Fig. 1b): one with a variable width ranging between 110 and 150 mm, and 2,460 mm of length (Channel A), and the other two (Channels B and C) with a fixed width of 115 and 55 mm and a length of 2,460 and 1,480 mm, respectively. In the channels A and B there were, 14 and 12 double nozzle holders respectively, half in each side of the fan.

One of the main capability of this smart sprayer was the possibility to automatically vary the airflow generated thanks to the variation of both fan outlet section width, varying the amplitude of Channel A, and blade pitch. Through a dedicated tablet connected with the sprayer via Wi-Fi, the operator can act the H3O® system selecting among three defined widths for channel A (110, 130 and 150 mm) and four defined blades' pitch (20°, 25°, 30° and 35°). The changes in width of channel A are done by

181    means of the millimetric displacement of a piston arranged parallel to the fan axis. The

182    bladesø pitch is changed through an electric precision actuator proceeded on the

183    eccentric axes of the blades.

184    Specifically, the experimental work was focused on the characterization of the airflow

185    generated combining two channel A widths (110 and 150 mm) and three bladesøpitches

186    (20°, 25°, and 30°). In all cases the power take-off (PTO) speed (480 rev min$^{-1}$)

187    recommended by the manufacturer and the high fan gear speed, corresponding to a

188    gearbox factor of PTO to fan equal to 1:4, were used. The high fan gear is the most

189    usual for citrus application. A decrease of the fan gear speed would produce a reduction

190    in the values of air velocity (De Moor et al., 2002; Delele et al., 2005; Sozzi, 2011) but

191    without affecting the air velocity pattern (De Moor et al., 2002; Delele et al., 2005).

192    Therefore, because the objective of the work was to study the effect of the blade pitch

193    and the width channel just one value for this parameter was chosen throughout the trials.

194        *2.3. Air velocities and airflow rates in the outlet of the fan*

195    Airflow rate was measured at the edge of an outlet using a sampling grid suitably placed

196    to cover the whole outlet section as detailed by Garcerá et al. (2017b). A series of

197    measurement points was used on a grid of 3-point (evenly spaced across the width of

198    each channel A and B) by 36- and 42-points (evenly spaced along the perimeter of

199    channels A and B, respectively). Sampling points in these channels were located in the

200    empty space between nozzle holders. For the channel C there were 8 points located in

201    the middle of the channel evenly spaced along its perimeter (Fig. 2). In each point the

202    air velocity (m s$^{-1}$) was measured and the measurements were replicated twice for the

203    six configurations investigated. A total of 1,032 measurements were performed for the

204    characterization of air velocities and airflow rates at the fan outlet. For all the channels,

205    the average distance between sampling points along the channel was 200 mm.

206    A hot-wire anemometer (model VelociCalc Plus 8386A-M-GB, TSI Incorporated,

207    Minnesota, USA) was used to obtain the air velocity in each measuring point. The

208    measurements were conducted on a point-by-point manner and without interfering the

209    air flow behavior because only the sensor window was located horizontal to the soil and

210    facing the air outlet. The window sensor is placed in the tip of a telescopic probe of 7.0

211 mm of diameter. The length probe is 1,016 mm that allows the operator to be located at

212 enough distance of the air outlet and inlet. The sensor covered an air velocity range of

213 0.0 to 50.0 m s$^{-1}$, with an accuracy of ± 0.015 m s$^{-1}$, a resolution of 0.01 m s$^{-1}$ and a

214 measuring frequency of 1 Hz during 60 s. The modulus of the velocity $V$ (m s$^{-1}$)

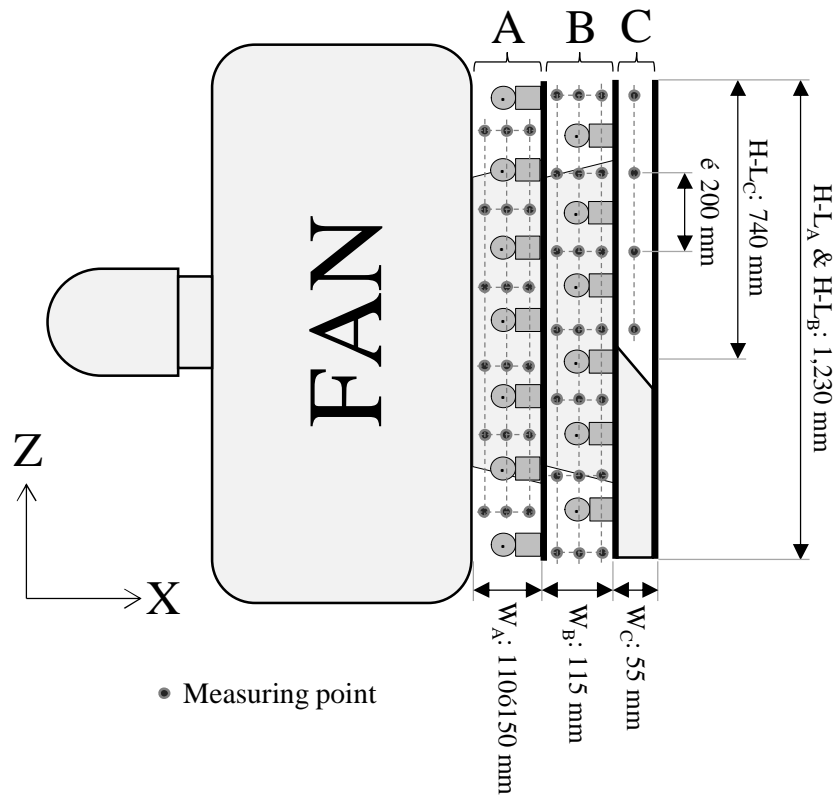215 perpendicular to the outlet was measured in each point.

216



217

218 **Fig. 2.** Elevation view of the measuring points positions to characterize airflow rate on

219 one side of the air outlet. The channels' dimensions are shown: width (W) and half-

220 length (H-L) of channels A, B and C. The average distance between sampling points

221 along the channel is indicated (≈ 200 mm).

222

223 After collecting data, the average air velocity in each point was calculated. Next, the

224 average air velocity on the right and left sides and both sides of the sprayer was

225 calculated as the mean of all measurements points of the grid corresponding to each part

226 and for the two repetitions. Following, airflow rate in each channel $Q_i$ (m$^3$ s$^{-1}$) was
227 calculated with Eq. (1):

228 $\qquad$ = + × $\qquad\qquad\qquad\qquad\qquad\qquad$ (1)

229 where $i$ is the corresponding channel (A, B, C), $V_R$ and $V_L$ (m s$^{-1}$) are the average air
230 velocity on the right and left side of the sprayer, respectively, in the corresponding
231 channel $i$, and $S_i$ (m$^2$) is the section of the corresponding channel $i$. The area occupied
232 by the nozzles was considered negligible compared to the total area of the channels.

233 When $Q_i$ was determined in each channel, then total airflow rate for each configuration
234 was obtained with Eq. (2):

235 $\qquad$ = $\sum$ $\qquad\qquad\qquad\qquad\qquad\qquad\qquad$ (2)

236 where $Q_T$ (m$^3$ s$^{-1}$) is the total airflow rate.

237 *2.4. Air velocity at different distances from the fan outlet*

238 The sprayer was placed in the middle of warehouse perpendicular to the longest axis,
239 with the tractor in the outside, to be sure that neither the walls nor the tractor affected
240 the air currents behavior in the sampling area. Outdoor windows and doors were kept
241 opened to minimize air overpressures from the walls or other undesirable inner
242 turbulences generated. Measuring points were always at a minimum distance of 1.5 m
243 from walls and roof to reduce any influence on the experimental data. Distance between
244 the sprayer air inlet and walls was larger than 3.0 m so that any effect of the walls on the
245 air inlet was negligible.

246 To characterize the main current coming out from the fan, the measurement points were
247 located in the path through which the main air streams circulated. Based on the results
248 obtained also from other authors (Salcedo et al., 2015, 2019; Triloff, 2016; Van de
249 Zande et al., 2017) the air current coming out from the fan of airblast sprayers is not
250 perpendicular to the outlet. Therefore, firstly the angle between the main direction of the
251 airflow and the perpendicular to the fan outlet was assessed, in both cases respect to the
252 fan outlet centre and in a plane parallel to the ground. The above-mentioned
253 measurements were conducted moving the hot-wire anemometer in parallel to the main

10

254 axis of the sprayer at different distances from it, at around 1.2 m above the ground, in
255 order to detect the points where the highest velocities occurred and distance reach by the
256 air jet. This was performed for both sprayer sides and for the six fan configurations
257 tested. It was found an average angle of 18° towards the advance direction of the
258 sprayer irrespective of sprayer side and that at 10 m the airjet was still noticiable which
259 may have implications for spray drift. Therefore, wind characteristics were measured
260 using a sampling grid located over the reference line defined by the angle prior obtained
261 for each configuration and sprayer side. Thus, the sides were labelled *L* for the left side
262 of the fan outlet and *R* for the right side (viewing the sprayer from the rear) (Fig. 3).
263 Sampling grids were placed at 1.0, 3.0, 5.0 and 10.0 m distances from the sprayer
264 corresponding to *L1, L3, L5* and *L10,* and *R1, R3, R5* and *R10* for the left and right
265 sides, respectively (Fig. 3).

266 At each distance, air velocity was recorded in three positions over a line running parallel
267 to the sprayer: a central position ($X = 0$ $m$), over the reference line, and two other
268 positions, located 0.30 m toward ($X = +0.30$ $m$) and backward ($X = ó0.30$ $m$) the
269 advance direction of the sprayer. In each of these positions, measurements were
270 performed at different heights from the ground. The first two measurements were
271 carried out at a height of 0.25 m and 0.5 m above the ground. From 0.5 m upwards, air
272 velocity was measured at 0.5 m intervals, up to a height of 4.0 m (Fig. 4).

273



274
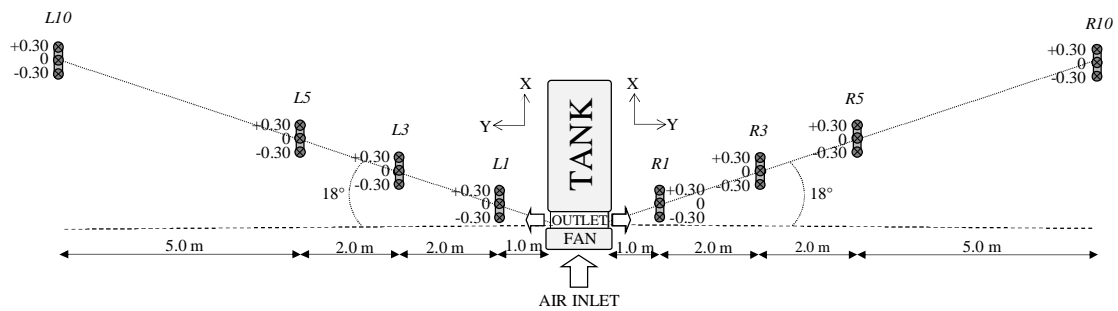
275 **Fig. 3.** Plan view of the layout of the measuring points to characterize air velocities.

276

11

L10   L5   L3   L1   FAN   R1   R3   R5   R10

4.0 m   4.0 m   4.0 m   4.0 m   4.0 m   4.0 m   4.0 m   4.0 m

Z   Y   0.5 m   0.25 m   0.25 m

5.0 m   2.0 m   2.0 m   1.0 m   1.0 m   2.0 m   2.0 m   5.0 m
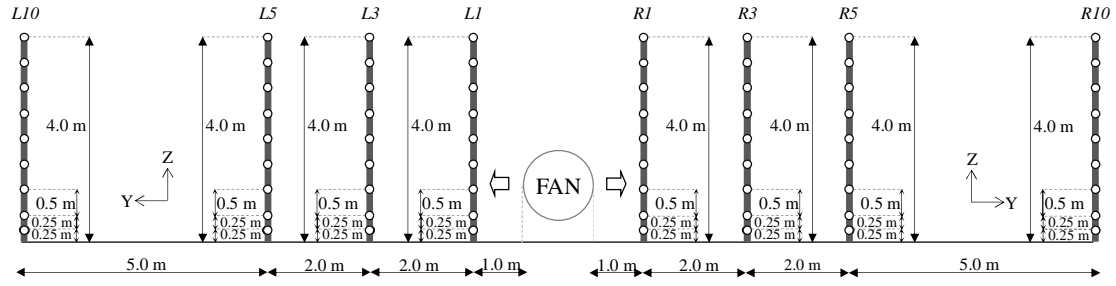
**Fig. 4.** Elevation view of the measuring plan in each plane ($X = -0.30$, $X = 0$, and $X = +0.30$ m).

A three-dimensional (3D) ultrasonic anemometer (WindMaster 1590-PK-020, Gill Instruments Ltd., Hampshire, UK) attached to a metal pole was placed in a vertical position, with the North of the sensor facing away from the sprayer. The sensor accuracy was 1.5%, with an air velocity range of 0.0 to 50.0 m s$^{-1}$ and a resolution of 0.01 m s$^{-1}$. The acquisition time was 60 s at every point, with a measuring frequency of 1 Hz. The three instantaneous components of air velocity ($u_x$, $u_y$, $u_z$) (m s$^{-1}$) were recorded. The positive $X$-axis was the horizontal direction parallel to the main axis of the sprayer and in the advance direction of the sprayer; the positive $Y$-axis was the horizontal direction perpendicular to the main axis of the sprayer and moving away from the sprayer (therefore, it had an opposite sign on each fan side); and the positive $Z$-axis was the vertical direction, directed upwards. In total, the air velocity was measured in 216 points for each configuration (2 fan sides $\times$ 4 distances/side $\times$ 3 positions/distance $\times$ 9 heights/position).

The air temperature and relative humidity were recorded during the experiment by means of a thermo-hygrometer (Log32, Data logger, Dostmann Electronic GMBH, Wertheim-Reicholzheim, Germany). The sensor was positioned at 4.5 m high out of reach of the air generated by the fan. Variables were measured at 0.5 Hz frequency.

### 2.4.1. Response variables

The influence of blade pitch and channel A width on airflow currents was studied over six response variables:

i) Magnitude of the vectors          :

12

(m s$^{-1}$) at each point is the average of the magnitude of the instantaneous vectors contained in the plane *YZ*, perpendicular to the sprayer which moves away from the fan, over the 60 s of the acquisition time (*n*) and was calculated with Eq. (3):

$$= -\sum \qquad (3)$$

Where   (m s$^{-1}$) is the magnitude of the instantaneous velocity vector in the measuring point at a specific time *i* and was calculated with the Eq. (4):

$$= \overline{\quad +\quad} \qquad (4)$$

ii) Angle of the vectors    :

(°) at each point is the average of the angles of the instantaneous vectors contained in the planes *YZ* with respect to the planes *YX*, parallel to the ground, during the 60 s of the acquisition time (*n*) and was calculated with Eq. (5):

$$= -\sum \qquad (5)$$

Where   (°) is the angle of the instantaneous velocity vector     in the measuring point at a specific time *i* in the planes *YZ* with respect to the horizontal planes *YX* and was obtained with the Eq. (6):

$$= \quad - \qquad (6)$$

iii) Magnitude of the vectors    :

(m s$^{-1}$) at each point is the average of the magnitude of the instantaneous vectors contained in the plane *ZX*, parallel to the sprayer, over the 60 s of the acquisition time (*n*) and was calculated with Eq. (7):

$$= -\sum \qquad (7)$$

Where $u_x u_z$ (m s$^{-1}$) is the magnitude of the instantaneous velocity vectors in the measuring point at a specific time *i* and was calculated with Eq. (8):

$$= \overline{\quad} + \quad \tag{8}$$

iv) Angle of the vectors :

(°) at each point is the average of the angles of the instantaneous vectors contained in the planes *ZX* with respect to the planes *YX*, parallel to the ground, during the 60 s of the acquisition time (*n*) and was calculated with Eq. (9):

$$= -\sum \tag{9}$$

Where (°) is the angle of the instantaneous velocity vectors , in the measuring point at a specific time *i* in the planes *ZX* with respect to the planes *YX* and was obtained with Eq. (10):

$$= \quad \overline{\quad} \tag{10}$$

v) Magnitude variation ratio $R_{ab}$ of the vectors *ZY*

The magnitude variation ratio $R_{ab}$ (%) of the vectors *ZY* is the gradient of velocity at a specific height between two consecutive distances to the fan, *a* and *b*, considering the main advance direction of the airflow current moving away from the sprayer, that is, between 1.0 m and 3.0 m, between 3.0 m and 5.0 m, and between 5.0 m and 10.0 m, respectively, and was calculated with Eq. (11):

$$= \overline{\quad} \times 100 \tag{11}$$

Where $U$ (m s$^{-1}$) is the total mean magnitude of the air velocity vector at one point and was calculated as the average of the instantaneous magnitude during the 60 s of the acquisition time (*n*) with Eq. (12):

$$= -\sum \tag{12}$$

Where $u$ (m s$^{-1}$) is the magnitude of the instantaneous air velocity at a measuring point at a specific time *i* and was obtained through the three components of the air velocity ($u_x$, $u_y$, $u_z$) with Eq. (13):

$$= \overline{\quad} + \quad + \quad \tag{13}$$

14

350     vi) The total turbulence intensity *I*.

351     *I* (%) is the turbulence intensity and is used to express the influence of the air
352     fluctuations on the mean velocity and was calculated with the Eq. (14):

353     $$= \frac{}{} \times 100 \tag{14}$$

354     Where:

355     -   $U$ (m s$^{-1}$) is the total mean magnitude of the air velocity vector (Eq. (12)).
356     -   $u\phi$ (m s$^{-1}$) is the total fluctuation considering the three components and it was
357         estimated by following Eq. (15):

358     $$= \overline{\phantom{xxxxxxxxxxxxx}} \phantom{x} + \phantom{xx} + \tag{15}$$

359     Where      ,      and      were respectively the mean square of the fluctuation in
360     each component of the space (Pope, 2000), which in this case is expressed as the
361     product      . In each component, the fluctuation of the air velocity      (m s$^{-1}$) in a
362     measuring point at a specific instant was defined as the difference between the specific
363     mean magnitude $U_i$, and the velocity $u_i$ in that moment (instantaneous velocity) (Eq.
364     (16)):

365     $$= \phantom{x} - \tag{16}$$

366         2.4.2.  Data processing and statistical analyses

367     The stability of the airflow at each measuring point was studied. Firstly, the evolution of
368     the magnitude $U$ during the 60 s of logging was plotted. It was observed that the values
369     were keeping the same order of magnitude and contained in the same range of velocities
370     (about $\pm 1.0$ m s$^{-1}$ as maximum approximately), as the acquisition time passed. Then, it
371     was checked that air velocities accomplished a quasi-steady flow (Rao et al., 2018). For
372     that, data of each point should fulfilled the following two requirements:

373     •   Maximum and minimum values of $U(i)$ during the last third of the measurement
374         time (20 s) of the acquisition time should be contained within the interval
375         formed by the total mean $U \pm$ standard deviation ($S_U$), as Eq. (18) expresses:

15

376    $\quad - \quad \leq \quad \leq \quad \leq \quad +$   (18)

- Coefficients of variation *CV* (%) among *U(i)* values calculated every 10 s (Eq. (19)) should be below an arbitraty value of 30% (Salcedo et al., 2015).

379    $$ = \dfrac{\quad\quad}{-\Sigma\quad ( )} $$   (18)

where        was the standard deviation within the 10 s of the corresponding interval.

All data in each measuring point were within these parameters, therefore the airflow was considered behaving as quasi-steady regime and it was proceeded the final analysis for the description of the flow.

The data were tested for normality using the Shapiro-Wilk test and by visual assessment of the Q-Q plots of Z-scores. Residuals analyses were also performed. The effect of the two first-level main factors (fan blade pitches and Channel A width) and the three sub-factors (height, distance, and side of the sprayer) on the magnitude and angle of vectors in the planes *ZY* and *ZX* were analyzed using multifactor analysis of variance (Multifactor ANOVA) with a confidence level of 95%. Up to the four-way interactions were studied. An iterative process was followed in which all the factors and their interactions were included. The effect with the highest non-significant p-value ( > 0.05) was removed and the model was recalculated. Only the effects with the highest significant level that include a main factor are interpreted in results.

An equation to explain the variation of air speed with the distance to the sprayer was obtained to ease the practical application of this study for regulating the fan sprayer. Because the phenomenon is very complex and there are too many measurements in different planes and heights, the data used to obtain the equations were selected in order to study the air speed where citrus trees are wider and denser, and therefore, more difficult to be penetrated by the air, that is, at the half-height of the canopy, which in Spain results in a height of 1.5 m above the ground (internal database of citrus characteristics). Moreover, only the data in *X=0* was used, because it is the position where the main current coming out from the sprayer was found. First of all, raw data

404 were plotted to determine which type of relationship existed between the magnitude of

405 each component of the air velocity vector ($u_X$, $u_Y$, $u_Z$, m s$^{-1}$) and the distance to the

406 sprayer ($D$, m), and to know if any transformation of the data would be necessary. Once

407 it was determined, Multiple Linear Regression (MLR) was used to model the

408 relationship between the variables. To study if the blades pitch, channel A width and/or

409 sprayer side affected the relationship, they were included as dummy variables, as well

410 as their interactions with the rest of variables. A dummy variable takes the value 0 or 1

411 to indicate the absence or presence of a categorical effect that may be expected to shift

412 the outcome. When a dummy variable has $n$ categories, only ($n$-1) dummy variables are

413 introduced to avoid multicollinearity. The category for which the dummy is not assigned

414 is known as the base group (Suits, 1957; Gujarati, 2003). In this study, dummy variables

415 called $I_{PITCH\_25}$ and $I_{PITCH\_30}$ were included to study differences in the relationship

416 between the main variables due to the blades pitch. They took the value 1 for the

417 experimental data corresponding to blades pitch 25° and 30°, respectively and 0

418 otherwise. Another dummy variable called $I_{WIDTH\_110}$ was included to study differences

419 due to the channel A width, which took the value 1 for the experimental data

420 corresponding to channel A width of 110 mm and 0 otherwise. Finally, a dummy

421 variable called $I_{RIGHT}$ was included to study differences due to the sprayer side, which

422 took the value 1 for the experimental data corresponding to the right side of the sprayer

423 and 0 otherwise. The variables for the most significant model were selected with the

424 forward method. When the dummy variables were found significant, the model could be

425 expressed as a set of equations that depended on the blades pitch, channel A width

426 and/or sprayer side. Quadratic effect of the explanatory variables was studied by means

427 of residual plots. One MLR model was generated for each velocity component. In all

428 fitted models, all the assumptions of linear regression were checked. No outliers were

429 identified.

430 All statistical analysis were performed with Statgraphics Plus 5.1 (Statpoint

431 Technologies, Inc., The Plains, Virginia, USA).

432

433

434 **3. Results and discussion**

435 *3.1. Air velocities and airflow rates at the outlet of the fan*

436 For all blade pitches tested, the narrower the outlet section, the greater the air velocity

437 (Table 1) as it was also observed by Sozzi (2011). This phenomenon was explained by

438 the principle of mass conservation: at a same fan setup conditions (480 rev min$^{-1}$, blade

439 pitch selected), a reduction in the outlet section (Channel A) from 150 to 110 mm was

440 compensated by an air velocity increment after passing through this section.

441 Nevertheless, a reduction of the exit channel also produced greater energy losses on the

442 fluid movement, due to a higher air friction against solid obstacles, which resulted in a

443 drop of the outgoing airflow. Furthermore, with both Channel A widths, higher air

444 velocities were found on the right side of the sprayer than on the left one. This stated the

445 asymmetric character of the fan.

446 It is known that as the blades' pitch increase, the rotational resistance of the fan increase.

447 However, in this study the PTO speed was maintained constant at 480 rev min$^{-1}$ for each

448 fan configuration, therefore the increase of fan resistance produces an increase in the

449 torque but it does not affect the air velocity and flow rate. In the experiment it was

450 observed that, by increasing the blades pitch from 20° to 30°, velocities raised and,

451 therefore airflow rates increased because as the bladesø pitch increased, the thrust

452 capacity of the blades raised as well. This effect was associated with a decrease in the

453 differences on velocities and airflow rates generated by the fan between the two sides.

454 On the other hand, an increase in the blades pitch also produced a gradual increment in

455 the variability of the air velocity. As the velocities grew, the fluctuations experienced by

456 the airflow were also greater. These results are in accordance with the ones obtained by

457 Sozzi (2011) and García-Ramos et al., (2012).

458

459 **Table 1.** Air velocity and airflow rate (mean (standard deviation)) in the fan outlet for
460 each combination of Channel A width and blades pitch, for each side of the sprayer.
461 Light grey coloured bars represent velocities and dark grey is for airflow rates. The
462 percentage of the airflow rate of each side of the sprayer is indicated.

| Blades pitch (°) | Sprayer side | Channel A width = 110 mm | | | Channel A width = 150 mm | | |
|---|---|---|---|---|---|---|---|
| | | Air velocity (m s$^{-1}$) | Airflow rate (m$^3$ h$^{-1}$) | Percentage rate (%) | Air velocity (m s$^{-1}$) | Airflow rate (m$^3$ h$^{-1}$) | Percentage rate (%) |
| 20 | Left | 21.9 (6.7) | 25,164 (727) | 47.6 | 21.3 (5.9) | 28,980 (232) | 47.9 |
| | Right | 24.0 (6.4) | 27,648 (285) | 52.4 | 23.4 (5.1) | 31,572 (337) | 52.1 |
| | TOTAL | 23.0 (6.6) | 52,812 (1,013) | 100.0 | 22.4 (5.5) | 60,552 (569) | 100.0 |
| 25 | Left | 28.3 (7.7) | 32,544 (608) | 48.2 | 24.3 (6.1) | 36,648 (465) | 48.6 |
| | Right | 30.4 (6.9) | 34,956 (660) | 51.8 | 28.9 (5.3) | 38,700 (419) | 51.4 |
| | TOTAL | 29.4 (7.3) | 67,500 (1,268) | 100.0 | 28.1 (5.7) | 75,348 (885) | 100.0 |
| 30 | Left | 32.7 (7.6) | 37,476 (389) | 48.7 | 30.5 (6.7) | 41,184 (386) | 48.7 |
| | Right | 34.4 (7.3) | 39,492 (462) | 51.3 | 32.4 (5.5) | 43,416 (374) | 51.3 |
| | TOTAL | 33.5 (7.4) | 76,968 (850) | 100.0 | 31.5 (6.2) | 84,600 (760) | 100.0 |

463
464

465 *3.2. Behavior of air velocity vectors at different distances from the fan*

466 During the measurements, the mean air temperature was 15.0 °C, with a minimum of
467 12.3 °C and a maximum of 18.3 °C. The mean relative humidity was 41.6%, with a
468 minimum of 33.0% and a maximum value of 50.9%. Differences in the air conditions
469 were considered negligible and without effect on the measurements.

470 Firstly, the air velocity vectors of the components in the planes *ZY* for *X = 0*, *X = -0.30*,
471 and *X = +0.30 m* and the effect of blades pitch and the Channel A width are described.
472 Secondly, the same parameters are shown in the *ZX* planes for *Y = 1*, *Y = 3*, *Y = 5*, and *Y*
473 *= 10 m*.

474 3.2.1 <u>ZY planes</u>

475 *3.2.1.1 Data in X = 0 m*
476 In this plane, the fan blades pitch had a significant influence on the magnitude of the *ZY*
477 vectors depending on the distance to the fan and the height (Table 2). Furthermore, this
478 factor affected the magnitude of the *ZY* vectors in interaction with the Channel A width
479 depending on the one hand on the height, and on the other hand, on the side of the
480 sprayer (Table 2). In this plane, the angle of the *ZY* vectors was also affected by the fan
481 blades pitch in interaction with the distance to the fan, the height and the side of the
482 sprayer (Table 3). The width of the channel A had a significant influence both on the

483 magnitude and the angle of the *ZY* vectors, depending on the distance to the fan, the
484 height, and the side of the sprayer (Fig. 5; Table 2; Table 3).

485

486 **Table 2.** Significant interactions from the Multifactor ANOVA for the magnitude of *ZY*
487 vectors in the planes *X=0 m*, *X=-0.30 m* and *X=+0.30 m*. The main factors have been
488 highlighted in bold.

| *X* Plane | Interactions | *F* | df | *P* |
|---|---|---|---|---|
| *0 m* | **Blades pitch** × Distance × Height | 3.22 | 48, 431 | 0.0001 |
| | **Blades pitch** × **Channel A width** × Height | 3.42 | 16, 431 | 0.0025 |
| | **Blades pitch** × **Channel A width** × Side | 3.14 | 2, 431 | 0.0457 |
| | **Channel A width** × Distance × Height × Side | 5.81 | 24, 431 | < 0.0001 |
| *-0.30 m* | **Blades pitch** × Distance × Height | 3.14 | 48, 431 | 0.0001 |
| | **Blades pitch** × Distance × Side | 3.32 | 6, 431 | 0.0039 |
| | **Blades pitch** × Distance × **Channel A width** | 5.20 | 6, 431 | 0.0001 |
| | **Channel A width** × Distance × Height × Side | 11.27 | 24, 431 | < 0.0001 |
| *+0.30 m* | **Blades pitch** × Distance × Height | 3.42 | 48, 431 | 0.0093 |
| | **Blades pitch** × Distance × **Channel A width** | 3.13 | 6, 431 | 0.0059 |
| | **Channel A width** × Distance × Height × Side | 8.29 | 24, 431 | < 0.0001 |

489
490 **Table 3.** Significant interactions from the Multifactor ANOVA for the angle of *ZY*
491 vectors in the planes *X=0 m*, *X=-0.30 m* and *X=+0.30 m*. The main factors have been
492 highlighted in bold.

| *X* Plane | Interactions | *F* | df | *P* |
|---|---|---|---|---|
| *0 m* | **Blades pitch** × **Channel A width** × Height × Side | 1.50 | 48, 431 | 0.0400 |
| | **Channel A width** × Distance × Height × Side | 7.98 | 24, 431 | < 0.0001 |
| *-0.30 m* | **Channel A width** × Distance × Height × Side | 3.37 | 24, 431 | < 0.0001 |
| *+0.30 m* | **Blades pitch** × **Channel A width** × Side | 3.64 | 2, 431 | 0.0400 |
| | **Blades pitch** × Distance × Height × **Channel A width** | 1.70 | 48, 431 | 0.0093 |
| | **Channel A width** × Distance × Height × Side | 2.87 | 24, 431 | 0.0001 |

493

494
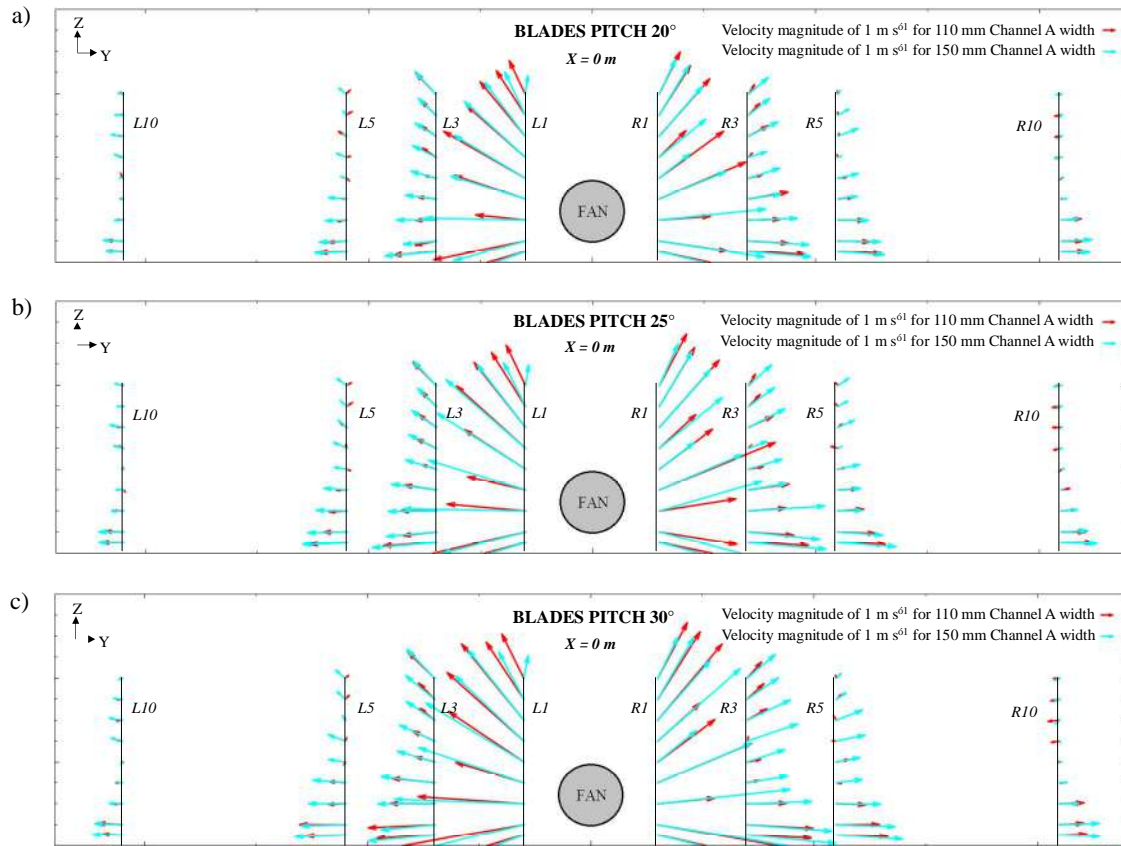


**Fig. 5.** *ZY* Air velocity vectors in the plane *X = 0 m* for each width of Channel A (110 and 150 mm) and blades pitch (20° (a), 25° (b) and 30° (c)). Vectors are shown for each distance.

It can be observed that vectors in *L1* and *R1* exhibited an air current whose vertical component was negative up to approximately 1.0 m height, coinciding with the middle zone of the fan. Then this vertical component became positive as well as bigger than the horizontal component in the *ZY* vectors, which was reducing as it moved away from the fan (Fig. 5).

On the left side, the profile obtained in *L1* offered a similar trend for both widths of the outlet section: velocities grew between 0.25 and 0.5 m heights, then reduced between 1.0 and 1.5 m, grew back between 2.0 and 2.5 m, and finally, minimized again at the furthest heights. Meanwhile, on the opposite side, in *R1*, the velocity vectors behaved similarly up to 2.5 m height. After this height, vectorsømagnitude grew up to 3.0 m and then decreased anew 4.0 m. The airflow profile reflected the differences between both

sides of the fan, according with the profile described in other studies with air-assisted sprayers (Salcedo et al., 2015, 2019; Triloff, 2016; Van de Zande et al., 2017). This character also corresponded with vectors studied in $X = -0.30\ m$ for *L1* and *R1* (Fig. 6), although with velocity vectors of greater magnitude in this plane. The height where these maximum and minimum velocities were found depended on the width of Channel A and the fan blades' pitch. In general, it was observed that the larger the fan blades pitch and the outlet section, the greater the velocities, and the lower the differences between heights up to 2.5 m, especially in *L1*. From 3.0 m height, velocity was reduced with bigger intensity in *L1* when the Channel A had a width of 150 mm.

At 3.0 and 5.0 m away from the fan, vectors magnitude with the 150 mm Channel A width always were higher than those measured with the 110 mm width. The horizontal component of the velocity vectors with the 150 mm Channel A width was always positive, while with the 110 mm Channel A width vectors were directed towards the sprayer in *L5* and *R5* between 2.0 and 2.5 m. At the distance *L10*, the influence of the fan could still be observed, with the vectors showing a positive horizontal component and moving away the fan, especially with the largest outlet section and the blades pitch of 30°. Meanwhile, in *R10* it was observed that velocities had a positive horizontal component until 1.0 m in height but from this height up there was a negative horizontal trend suggesting the presence of a vortex. The airflow was reduced closer to the fan with 110 mm than with 150 mm Channel A width, and more noticeably on the right side than on the left, regardless of the pitch of the fan blades.

The air currents found at 10.0 m distance from the fan implies that drift would reach this distance even in the absence of wind, just by the effect of the sprayer fan. This also explain the considerable drift amount found in citrus at this distance and onwards (Torrent et al., 2017). Therefore, these results could be useful for managing drift through the regulation of the fan. It is expected that with 110 mm Channel A width and with 20° blade pitch drift would be lower.

Considering $X = 0\ m$ such as the plane lined up with the main air stream, in general it was observed that there was a less presence of the airflow for 110 mm at the different distances, from 1.0 to 10.0 m away. It could be explained for two reasons. One could be due to the principle of mass conservation: as the initial airflow was greater at 150 mm

541     width (Fig. 5), when the air current reached out the different distances, it kept having a

542     greater physical presence than the air stream at 110 mm, which implied larger vectors

543     registered with 150 mm in general. The second reason would be related with how the air

544     stream was expanding as the air left Channel A. Data in Fig. 6 (plane $X = -0.30\ m$)

545     indicated that the air with 110 mm width was distributing more to the sides as well it

546     was moving away from the sprayer.

547     *3.2.1.2 Data in $X = -0.30\ m$*

548     The fan blades pitch had also a significant influence on the magnitude of the *ZY* vectors,

549     which depended on the distance to the fan and the height (Fig. 6; Table 2). Furthermore,

550     the fan blades pitch affected the magnitude of the *ZY* vectors depending on the distance

551     to the fan and the side of the sprayer (Table 2), and depending on the distance to the fan

552     and the Channel A width (Table 2). However, the blades pitch did not affect the angle of

553     the *ZY* vectors.

554     As it happened in the plane $X = 0\ m$, the width of the Channel A had a significant

555     influence both on the magnitude and the angle of the *ZY* vectors, and in both cases this

556     influence depended on the distance to the fan, the height and the side of the sprayer

557     (Fig. 6; Table 2; Table 3).

558

559
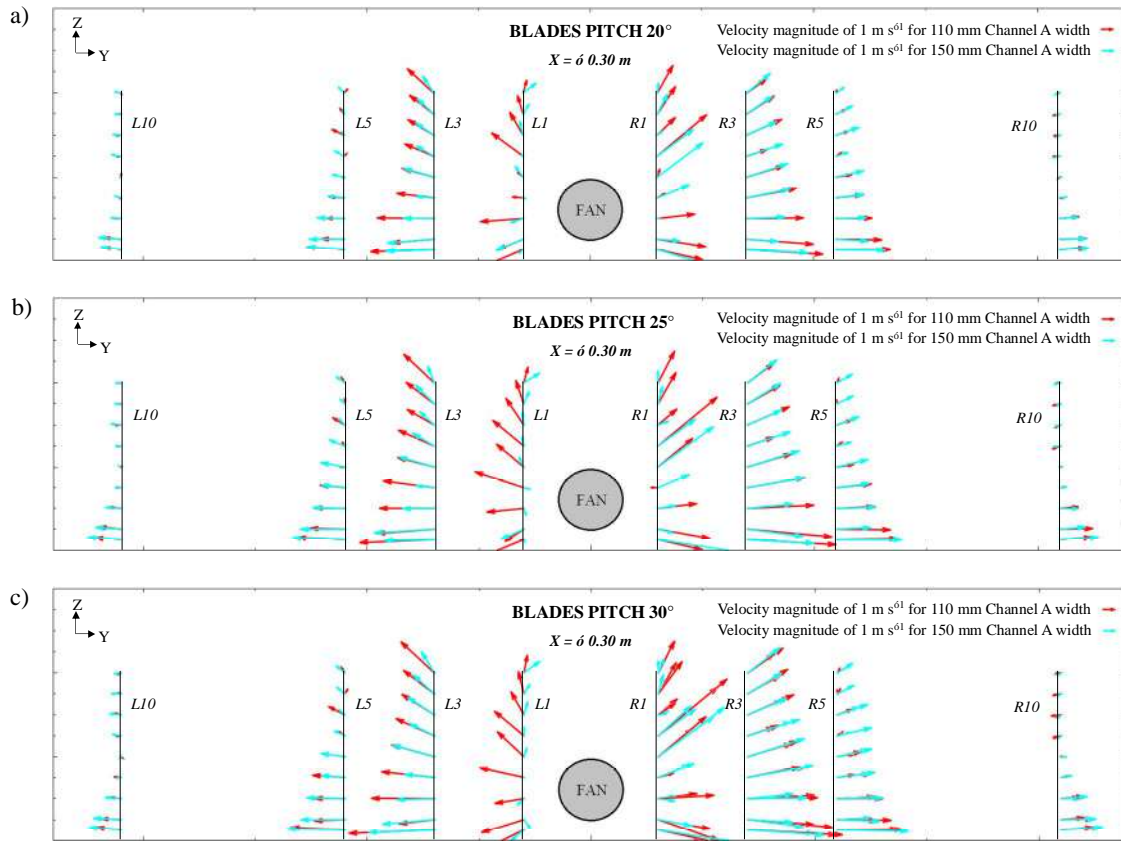


**Fig. 6.** *ZY* Air velocity vectors in the plane *X = -0.30 m* for each width of the Channel A (110 and 150 mm) and fan blades pitch (20° (a), 25° (b) and 30° (c)). Vectors are shown for each distance.

The general behavior of the vectors (direction, orientation, magnitude) at 1.0 and 3.0 m away from the sprayer shown how the air stream became wider when it left the outlet section (Fig. 6). The asymmetry of the fan was also notable, as the airflow opened unevenly on both sides. While in *L1* the magnitudes with 110 mm were higher, on the right side (*R1*) there were areas (velocity vectors corresponding to heights between 1.5 and 2.0 m) where the outgoing vectors with the 150 mm Channel A width had a magnitude more than twice bigger than with the 110 mm Channel A width. Regarding the velocity vectors up to a distance of 5.0 m from the fan, it was found that at the lowest height, vectors showed an orientation towards the ground, while in the higher positions, the velocity vectors had a positive vertical component. The asymmetric

24

575  differences were still present: meanwhile in *L5* the magnitude of the vectors from the

576  largest outlet section was greater than that of the vectors for the 110 mm Channel A

577  width, in *R5* this effect was only detected for heights bigger than 1.5 m. At 10.0 m from

578  the fan, there were still variations between the two sides of the sprayer. While on the left

579  side velocities had a positive horizontal component, on the right side this trend changed

580  after 1.0 m height. This indicated the presence of a turbulent structure in the form of

581  vortex perpendicular to the *ZY* plane (parallel to the sprayer direction). The general

582  orientation of the vectors at 10.0 m, together with data at 5.0 m, displayed that the air

583  current was still opening in this plane for both widths of Channel A. But the airflow

584  from a width of 110 mm was also losing more kinetic energy than at 150 mm at these

585  distances.

586  By increasing the blades pitch, the greatest variations with respect to the blades pitch of

587  20° were found in the distances closest to the fan and, therefore, most exposed to the

588  turbulences generated by the fan. The increase in the velocity of the outgoing air current

589  produced a rise in magnitude of the vectors. The differences among heights for the same

590  outlet section were minor. The trend of vectors up to 5.0 m from the fan were the same.

591  In all cases, the largest velocity vectors between 3.0 and 10.0 m distance were located in

592  the positions closest to the ground, matching with the fan height zone.

593  *3.2.1.3 Data in X = +0.30 m*

594  At the plane *+0.30 m*, the fan blades pitch had a significant influence on the magnitude

595  of the *ZY* vectors depending on the distance to the fan and the height and also depending

596  on the distance to the fan and the Channel A width (Table 2) as it happened at *-0.30 m*

597  plane. However, in this plane the angle of the *ZY* vectors was also affected by the blades

598  pitch in interaction with the side of the sprayer and the Channel A width and in

599  interaction with the distance to the sprayer, the height and the Channel A width (Table

600  3).

601  In this plane, the Channel A width produced an effect in the *ZY* vectors as happened in

602  the planes *X = 0* and *X = -0.30 m*. The Channel A width had a significant influence on

603  the magnitude and the angle of the *ZY* vectors, depending on the distance to the fan, the

604  height and the sprayer side (Table 2; Table 3).

25

605  In this plane, a general lower intensity of the magnitude of the vectors in *L1* and *R1*

606  (Fig. 7), compared to the other two planes (Fig. 6 and Fig. 5), is observed and it is due

607  to the fact the outgoing airflow opened more towards planes *X = -0.30 m*. On the left

608  side (*L1*), only the influence of the airflow generated by the fan was observed at 2.5 m

609  height, while on the right side (*R1*) it was from 3.0 m height, with the two components

610  of the velocity vectors with a positive direction. Velocities changed direction in the

611  remaining heights, coinciding with the height of the equipment tank, with the vectors

612  moving towards the sprayer. These vortexes were magnified with the increase in the fan

613  blades pitch and the reduction of the outlet section. The fan blades pitch increased also

614  the vertical component of the vectors at the highest heights. In *L3* these turbulent

615  structures were not registered, displaying the influence of the main outgoing airflow

616  from the fan, especially with the 150 mm Channel A width. This also happened in *R3*

617  with the same Channel A width, while with the 110 mm Channel A width turbulent

618  structures were again perceived from 2.0 m height. At a distance of 5.0 m from the fan,

619  similar airflow behavior was detected in both sides of the sprayer. The orientation of the

620  vectors in *L10* and *R10* was similar to the planes *X = 0 m* and *X = +0.30 m* (Fig. 5 and

621  Fig. 6).

622  Observing the vectors from 1.0 to 10.0 m, it can be deduced that the air stream with a

623  width of 150 mm was expanding more towards *X = +0.30 m* from 3.0 m than when the

624  fan was working with a width of 110 mm. Considering the other two *ZY* planes, it could

625  be deducted that with the smaller outlet cross section, the airflow was more focused in *X*

626  *= -0.30 m* and *X = 0 m*, while the airflow leaving from the large width was more

627  distributed among the planes, although there were always differences in the air profiles

628  between the two sides of the sprayer.

629  The behavior of the vectors collected in the three *ZY* planes, regardless the width of the

630  Channel A or the blade pitch, confirmed that the main air current of the fan followed a

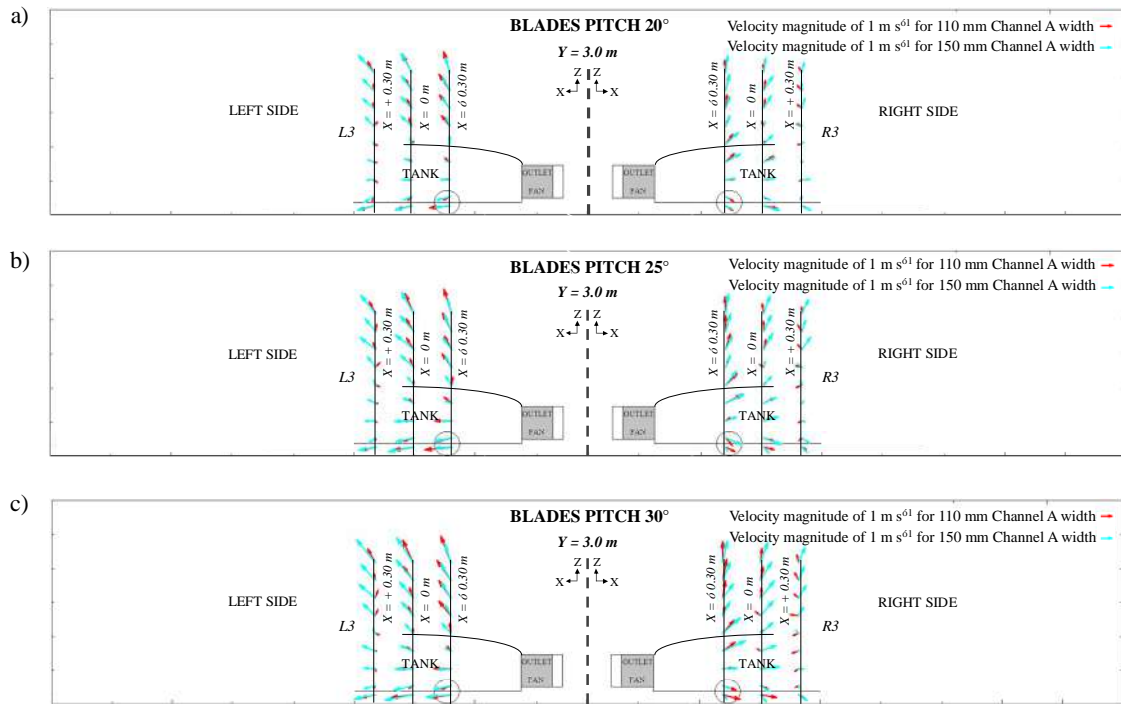631  deviated path towards the direction of advance of the sprayer (Fig. 3).

632

633



634
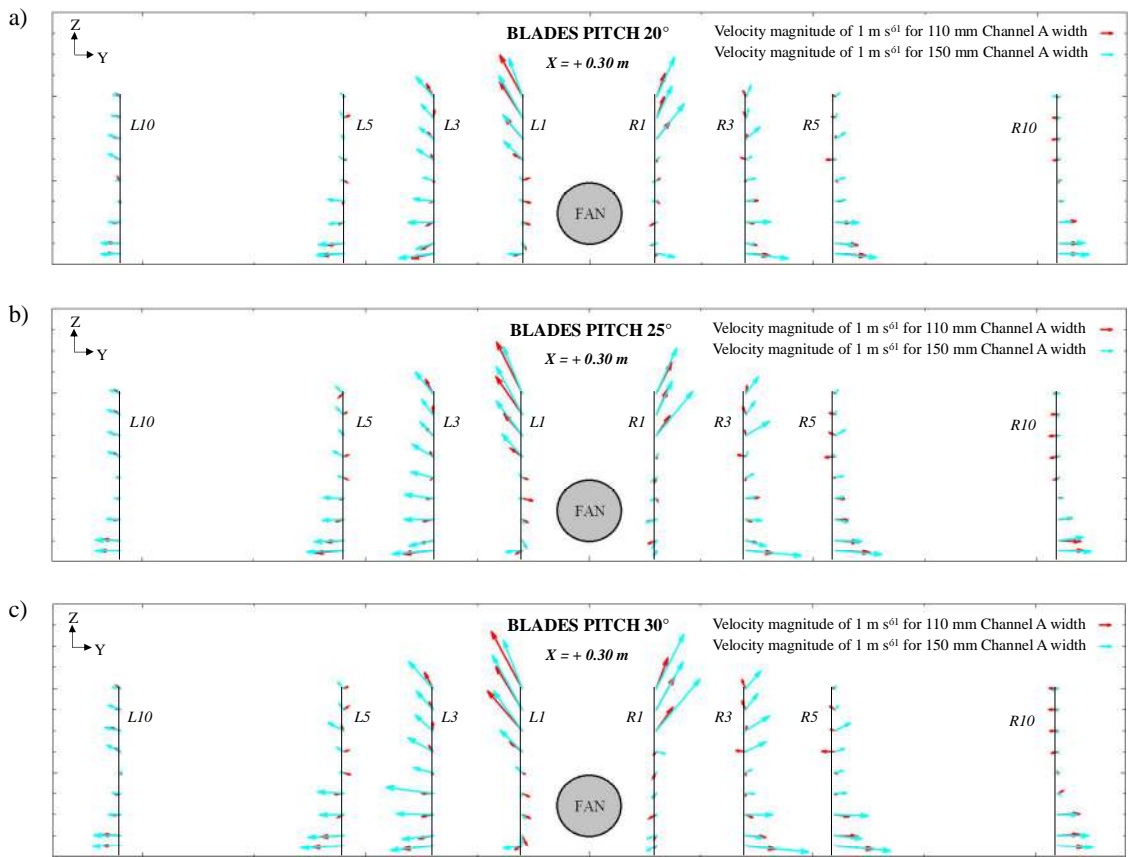
**Fig. 7.** *ZY* Air velocity vectors in the plane $X = +0.30$ *m* for each width of Channel A (110 and 150 mm) and blades pitch (20° (a), 25° (b) and 30° (c)). Vectors are shown for each distance.

638

### 3.2.2   ZX planes

*3.2.2.1* Data in *Y = 1.0 m*

The fan blades pitch had a significant influence on the magnitude of the *ZX* vectors depending on the width of the Channel A and the position (*X=0 m*; *X=-0.30 m*; *X=+0.30 m*) (Table 4). Also, the fan blades pitch affected the angle of the *ZX* vectors depending on the Channel A width, the height and the position (Table 5). Furthermore, the Channel A width had a significant influence on the magnitude and the angle of the *ZX* vectors, depending on the height, the position and the sprayer side (Table 4; Table 5; Fig. 8).

648

**Table 4**. Significant interactions from the Multifactor ANOVA for the magnitude of *ZX*

vectors in the planes *Y=1.0 m*, *Y=3.0 m*, *Y=5.0 m* and *Y=10.0 m*. The main factors have

been highlighted in bold.

| *Y* **Plane** | **Interactions** | *F* | df | *P* |
|---|---|---|---|---|
| *1.0 m* | **Blades pitch** × Position × **Channel A width** | 2.61 | 4, 323 | 0.0367 |
| | **Channel A width** × Height × Position × Side | 10.74 | 16, 323 | < 0.0001 |
| *3.0 m* | **Blades pitch** × Height × Position × Side | 1.74 | 32, 323 | 0.0298 |
| | **Blades pitch** × Height × Side × **Channel A width** | 3.93 | 16, 323 | < 0.0000 |
| | **Blades pitch** × Position × Side × **Channel A width** | 3.18 | 4, 323 | 0.0191 |
| | Height × Position × Side × **Channel A width** | 9.62 | 16, 323 | < 0.0000 |
| *5.0 m* | **Blades pitch** × Height × Side × **Channel A width** | 4.73 | 16, 323 | < 0.0001 |
| | Height × Position × Side × **Channel A width** | 4.24 | 16, 323 | < 0.0001 |
| *10.0 m* | **Blades pitch** × Height × Side × **Channel A width** | 1.70 | 16, 323 | < 0.0001 |
| | **Blades pitch** × Position × Side × **Channel A width** | 2.64 | 4, 323 | 0.0354 |

652

**Table 5.** Significant interactions from the Multifactor ANOVA for the angle of *ZX*

vectors in the planes *Y=1.0 m*, *Y=3.0 m*, *Y=5.0 m* and *Y=10.0 m*. The main factors have

been highlighted in bold.

| *Y* **Plane** | **Interactions** | *F* | df | *P* |
|---|---|---|---|---|
| *1.0 m* | **Blades pitch** × Height × Position × **Channel A width** | 3.09 | 32, 323 | < 0.0000 |
| | **Channel A width** × Height × Position × Side | 11.55 | 16, 323 | < 0.0001 |
| *3.0 m* | Height × Position × Side × **Channel A width** | 2.51 | 16, 323 | 0.0015 |
| *5.0 m* | **Blades pitch** × Height × Side × **Channel A width** | 1.95 | 16, 323 | 0.0182 |
| | Position × **Channel A width** | 9.48 | 2, 323 | < 0.0001 |
| | Height × Side × **Channel A width** | 6.27 | 8, 323 | < 0.0001 |
| *10.0 m* | **Blades pitch** × Height × Side × **Channel A width** | 2.11 | 16, 323 | 0.0109 |
| | **Channel A width** × Height × Side × Position | 2.82 | 16, 323 | 0.0009 |

656

In this plane, air currents in the positions *X = 0* and *X = -0.30 m* showed a positive

horizontal component towards the tractor (Fig. 8). The airflow had a more vertical

behavior with the 110 mm Channel A width than with the 150 mm width at the height

660    up to 1.5 ó 2.0 m. The largest velocities were registered at 1.0 - 1.5 m high with the

661    vectors following a direction more parallel to the equipment. By increasing the fan

662    blades pitch and therefore the airflow rate, the horizontal component gained more

663    presence than the vertical one. Observing also the results of *ZY* vectors at *X=0* in *L1* and

664    *R1* (Fig. 5), it could be noticed that at a greater outlet width and fan blades pitch, the air

665    currents arrived with higher magnitude at 1.0 m distance, but they were more diverted

666    towards the tractor. The heights where the maximum and minimum values were located

667    coincided with the profiles registered in *ZY* (Fig. 6, Fig. 5 and Fig. 7). In *X = +0.30 m*,

668    the presence of two vertical vortexes, one situated in each side of the sprayer, were

669    again appreciated, as in Fig. 7. The vortex axis of each one coincides with the tank

670    height. These vortexes will acquire more presence by decreasing the width of the

671    Channel A and increasing the blades pitch.

672



673
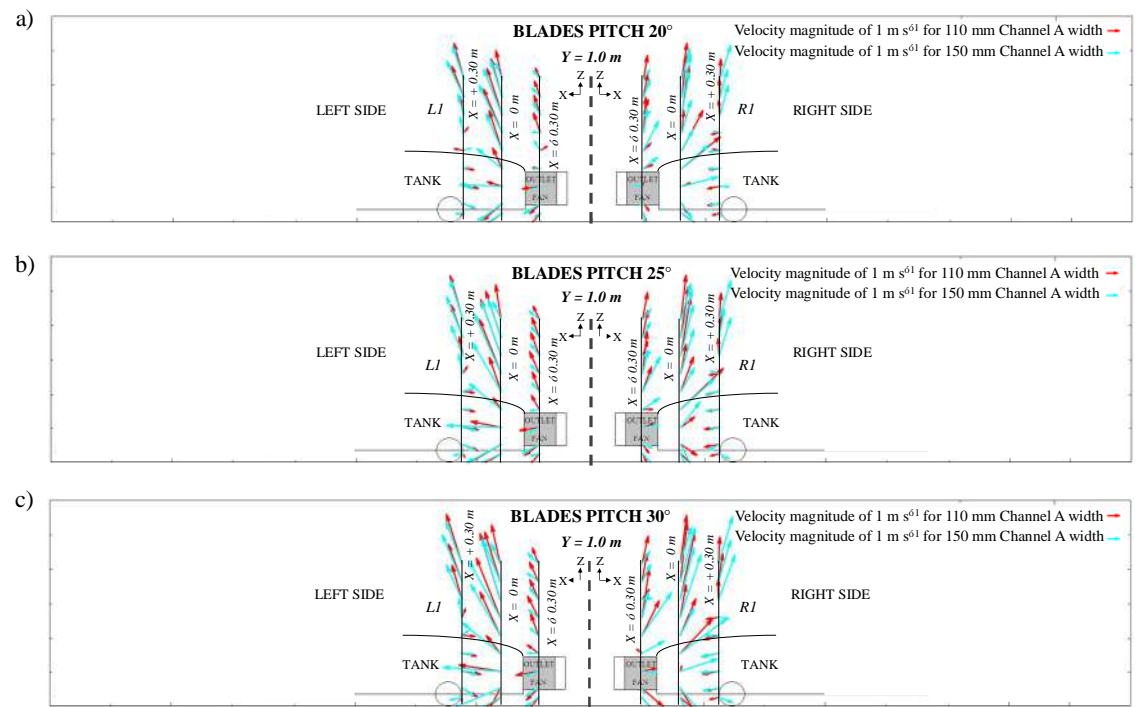
674    **Fig. 8**. *ZX* Air velocity vectors in the plane *Y = 1.0 m* for each width of Channel A (110

675    and 150 mm) and blades pitch (20° (a), 25° (b) and 30° (c)). Vectors are shown for each

676    distance.

677 *3.2.2.2 Data in Y = 3.0 m*

678 In this plane, the four interactions of order $4^{th}$ resulted statistically significant for the

679 magnitude of the *ZX* vectors (Table 4). Meanwhile, the angle of the *ZX* vectors was not

680 affected by the blades pitch but it was affected by the Channel A width depending on the

681 position, the height and the sprayer side (Table 5; Fig. 9).

682 Vectors in *X = -0.30 m* showed a positive horizontal component. Their magnitude

683 increased as the section of the fan outlet and the fan blades pitch increased (Fig. 9).

684 Vectors between 2.5 and 4.0 m heights showed a predominantly vertical behavior on the

685 right side of the sprayer. This meant that the velocity vectors were in a position

686 approximately perpendicular to the sprayer. This effect was greater with the 110 mm

687 Channel A width and by increasing the fan blades pitch. However, this did not happen

688 on the left side of the equipment, where the vectors were more directed towards the

689 tractor. At *X = 0 m*, the velocity vectors presented greater magnitude with the 150 mm

690 Channel A width. At the same time, the vectors had a positive horizontal component on

691 both sides of the equipment. But with the 110 mm Channel A width, some vectors in the

692 right side had an orientation opposite to the theoretical advance of the sprayer. These

693 deviations were present in more positions of *R3* with greater blades pitch. Finally, at *X*

694 *= +0.30 m*, vectors in the left side displayed a positive horizontal component only with

695 the 150 mm Channel A width. With the 110 mm Channel A width, which generated

696 smaller airflow rates, lower presence of the air current was noticeable. Under these

697 conditions, vectors had lower magnitude and were oriented towards the fan. On the left

698 side, only the velocity vectors generated with the 150 mm Channel A width showed

699 positive horizontal components at a height between 3.0 and 4.0 m. By decreasing the

700 outlet section and increasing the fan blades pitch, the asymmetry of the airflow

701 generated by the fan was more noticeable at 3.0 m distance, as it could be seen in *ZY*

702 planes (Fig. 5, Fig. 6 and Fig. 7).

703

a)
BLADES PITCH 20°

Velocity magnitude of 1 m s⁻¹ for 110 mm Channel A width
Velocity magnitude of 1 m s⁻¹ for 150 mm Channel A width

b)
BLADES PITCH 25°

Velocity magnitude of 1 m s⁻¹ for 110 mm Channel A width
Velocity magnitude of 1 m s⁻¹ for 150 mm Channel A width

c)
BLADES PITCH 30°

Velocity magnitude of 1 m s⁻¹ for 110 mm Channel A width
Velocity magnitude of 1 m s⁻¹ for 150 mm Channel A width

704

**Fig. 9.** *ZX* Air velocity vectors at the distance *Y = 3.0 m* for each width of Channel A (110 and 150 mm) and blades pitch (20° (a), 25° (b) and 30° (c)). Vectors are shown for each distance.

*3.2.2.3* Data in *Y = 5.0 m*

In this plane, the fan blades pitch had a significant influence on the magnitude and the angle of the *ZX* vectors, depending on the height, the sprayer side and the Channel A width (Table 4; Table 5). The Channel A width also affected the magnitude of the *ZX* vectors but depending on the height, the position and the side of the sprayer (Table 4). The angle of the *ZX* vectors also was affected by the Channel A width in interaction with the position and in interaction with the height and the side of the sprayer (Table 5; Fig. 10).

At 5.0 m from the fan, only the vectors at *X = -0.30 m* presented a positive horizontal component (except on the left side of the sprayer for the 110 mm Chanel A width at fan blade pitch of 20°), increasing its magnitude as the fan blades pitch augmented (Fig. 10). The vertical component of the vectors showed a value close to 0 m s⁻¹, which means that the airflow was mainly parallel to the ground. On the other hand, in the other two positions (*X = 0 m* and *X = +0.30 m*) only velocity vectors located within the first

31

723 0.5 m height also followed this trend. With the 150 mm Channel A width, vectors still

724 had a positive horizontal component in all three positions. In the rest of the heights,

725 velocity vectors had an erratic character and a smaller magnitude than in *Y= 3.0 m* (Fig.

726 9). As it happened in *ZY* planes at 5.0 m (Fig. 5, Fig. 6 and Fig. 7), the magnitude of the

727 vectors were higher close to the ground. The position of *X = -0.30 m* in the left side of

728 the fan showed the higher magnitudes. In *X = 0* and *X = +0.30 m*, velocity vectors

729 showed a more random orientation.

730

731
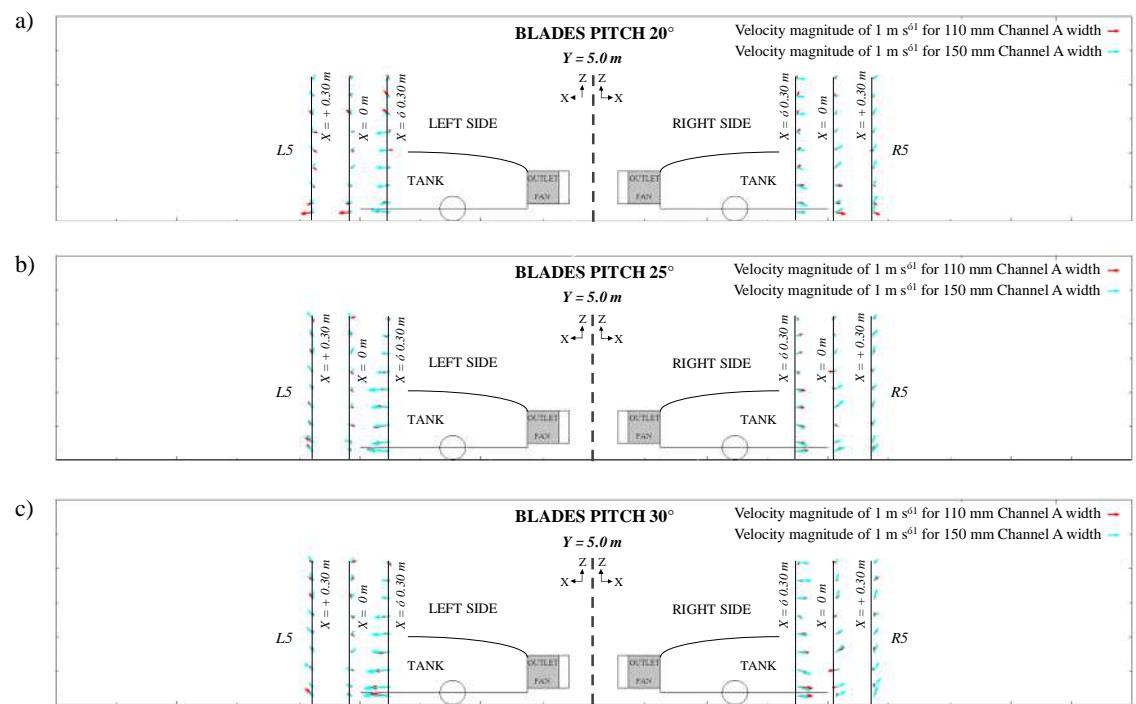


732 **Fig. 10.** *ZX* Air velocity vectors at the distance *Y = 5.0 m* for each width of Channel A

733 (110 and 150 mm) and blades pitch (20° (a), 25° (b) and 30° (c)). Vectors are shown for

734 each distance.

735

736 *3.2.2.4 Data in Y = 10.0 m*

737 In this plane, the 4th interaction between the fan blades pitch, the height, the sprayer side

738 and the Channel A width resulted statistically significant on the magnitude of *ZX* vectors

739 (Table 4) and its angle (Table 5). Furthermore, the magnitude of the *ZX* vectors was

740 affected by the fan blades pitch and the Channel A width in different way depending on

741 the position and the sprayer side (Table 4). The angle of the *ZX* vectors was also

742 affected by the Channel A width depending on the height, the position and the sprayer

743 side (Table 5; Fig. 11).

744 According to the data in the *ZY* planes in *L10* and *R10* (Fig. 5, Fig. 6 and Fig. 7), in

745 general only the vectors between 0.25 and 1.5 m heights followed the direction of the

746 outgoing current from the fan (Fig. 11). This behavior was most noticeable at *X = - 0.30*

747 *m*. The greater the Channel A width and the fan blades pitch, the bigger the magnitude

748 of these velocity vectors. The main component was the horizontal one. The magnitude

749 of these vectors was bigger on the left side of the sprayer. The vectors in the rest of the

750 points showed smaller magnitude. Comparing with the data at 1.0 m distance (Fig. 8), it

751 seemed that the airflow generated from the fan was no longer expanding within the *ZX*

752 direction, except in the nearest points to the ground.

753 The largest magnitude *XZ* vectors, from *Y = 1.0* to *Y = 10.0 m*, were generally oriented

754 toward the atmosphere. This could suggest the potential initial risk that axial fans have

755 in the generation of airborne spray drift. It seemed to be lower when selecting a width of

756 150 mm in Channel A and a blade pitch of 20° (less air velocity in the vicinity of the fan

757 outlet). Furthermore, these vectors were also following the advance direction of the

758 sprayer.
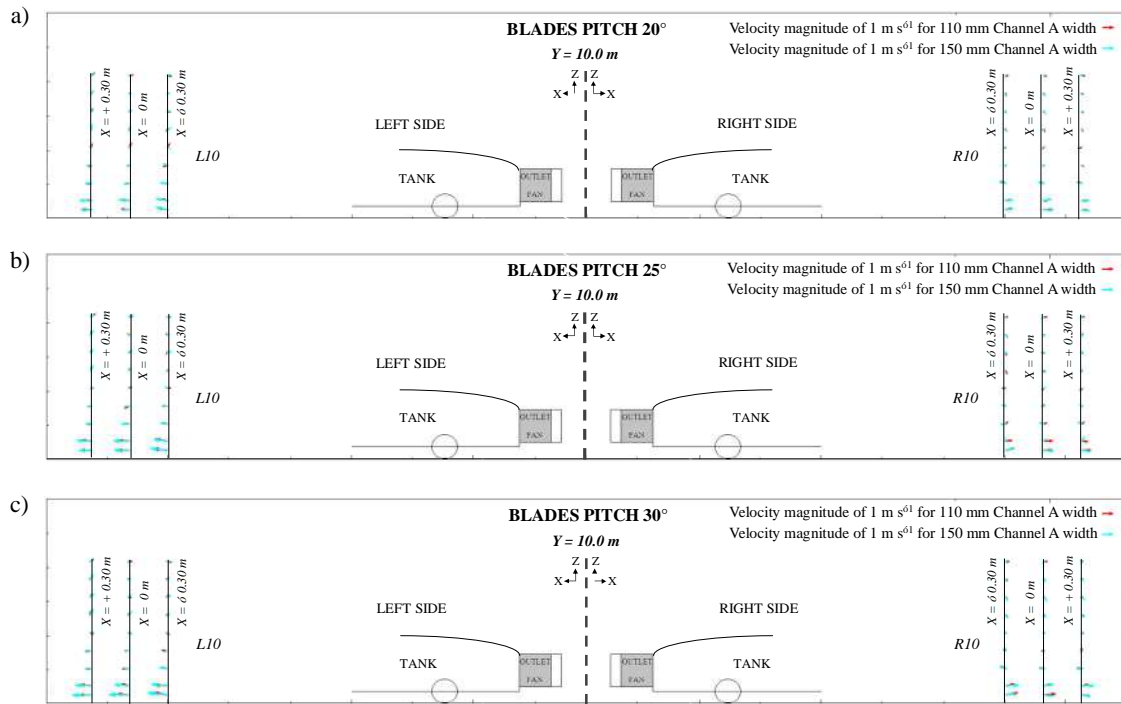
**Fig. 11.** *ZX* Air velocity vectors at the distance *Y = 10.0 m* for each width of Channel A (110 and 150 mm) and blades pitch (20° (a), 25° (b) and 30° (c)). Vectors are shown for each distance.
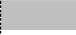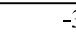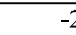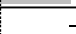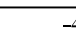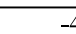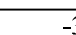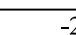
*3.3. Magnitude variation ratio ($R_{ab}$, %) for the vectors ZY between two consecutive distances to the fan and variation of air speed with the measurement distance to the sprayer*

The magnitude variation ratio for the vectors *ZY* between the distances 1.0 and 3.0 m from the fan was always negative in the central plane (Table 6). As it is showed in Fig. 6, the kinetic energy losses experienced by the airflow in that section is very intense on both sides of the equipment. This reduction in the velocity gradient was most noticeable with the 110 mm Channel A width, which generated the greatest initial air velocities in comparison with the 150 mm width. However, the variation of the fan blades pitch did not have effect in the magnitude variation ratios. In the plane *X = -0.30 m*, the gradients were positive, with the largest values for 150 mm Channel A width. At the same time, the ratios at *X = +0.30 m* showed a different behavior depending on the width of the channel A: negative for 110 mm and positive for 150 mm. This is in line with the

34

777 airflow deducted from the *ZY* planes: the air current were more distributed among

778 planes, unlike the air stream from 110 mm width located more in $X = -0.30\ m$ and $X = 0$

779 *m*.

780 In the interval between 3.0 and 5.0 m from the fan, negative ratios were present in most

781 situations (Table 6). These gradients were lower compared with the 150 mm Channel A

782 width than with 110 mm width. When the air current moved from 5.0 to 10.0 m from

783 the fan, for the 110 mm Channel A width, the greater negative ratios occurred in $X = -$

784 $0.30\ m$ and the lowest in the plane $X = + 0.30\ m$, and in general more marked on the left

785 side of the sprayer than on the right (except for blades pitch of 20° on the left side). In

786 contrast, for the 150 mm Channel A width, the gradient on the right side was greater and

787 the values were similar for the planes $X = 0\ m$ and $X = -0.30\ m$ and lower in the plane $X$

788 $= + 0.30\ m$.

789

790 **Table 6.** Magnitude variation ratio ($R_{ab}$, %) for the vectors *ZY* between two consecutive

791 distances to the fan from 1.0 to 10.0 m depending on the width of Channel A (110 and

792 150 mm) and fan blades pitch (20°, 25° and 30°). Coloured bars with light grey

793 represent positive values and dark grey is for negative ones.

| Channel A width (mm) | Blades pitch (°) | Plane X (m) | Sprayer side | Interval (m) | | |
|---|---|---|---|---|---|---|
| | | | | 1.0—3.0 | 3.0—5.0 | 5.0—10.0 |
| | | | | $R_{ab}$ (%) | $R_{ab}$ (%) | $R_{ab}$ (%) |
| 110 | 20 | - 0.30 | Left | 70.7 | -60.9 | -48.0 |
| | | | Right | 57.2 | -47.5 | -53.0 |
| | | 0 | Left | -64.4 | -47.0 | -30.6 |
| | | | Right | -61.0 | -34.1 | -37.4 |
| | | + 0.30 | Left | -10.3 | 6.2 | -24.8 |
| | | | Right | -22.7 | -18.2 | -19.8 |
| | 25 | - 0.30 | Left | 44.0 | -55.2 | -51.4 |
| | | | Right | 58.6 | -52.5 | -47.2 |
| | | 0 | Left | -58.6 | -50.8 | -35.4 |
| | | | Right | -63.8 | -33.0 | -29.1 |
| | | + 0.30 | Left | -11.9 | -13.4 | -18.8 |
| | | | Right | -13.7 | 8.7 | -19.7 |
| | 30 | - 0.30 | Left | 47.9 | -53.8 | -49.8 |
| | | | Right | 31.4 | -54.5 | -43.7 |
| | | 0 | Left | -59.1 | -52.8 | -37.8 |
| | | | Right | -64.8 | -28.2 | -30.7 |
| | | + 0.30 | Left | -18.1 | -8.5 | -24.0 |
| | | | Right | -15.1 | 0.3 | -9.7 |
| 150 | 20 | - 0.30 | Left | 87.0 | -37.0 | -36.9 |
| | | | Right | 64.2 | -32.1 | -57.3 |
| | | 0 | Left | -45.3 | -50.4 | -33.7 |
| | | | Right | -47.0 | -39.5 | -49.9 |
| | | + 0.30 | Left | 34.8 | -37.4 | -11.3 |
| | | | Right | 3.1 | 1.4 | -39.7 |
| | 25 | - 0.30 | Left | 99.0 | -22.8 | -45.9 |
| | | | Right | 70.6 | -37.3 | -58.1 |
| | | 0 | Left | -42.3 | -46.4 | -41.6 |
| | | | Right | -44.4 | -44.5 | -55.1 |
| | | + 0.30 | Left | 42.4 | -34.0 | -22.8 |
| | | | Right | 16.2 | -15.9 | -40.6 |
| | 30 | - 0.30 | Left | 115.0 | -34.1 | -42.8 |
| | | | Right | 63.8 | -31.4 | -59.9 |
| | | 0 | Left | -40.5 | -46.2 | -44.9 |
| | | | Right | -41.2 | -41.6 | -58.1 |
| | | + 0.30 | Left | 55.8 | -36.6 | -25.3 |
| | | | Right | 8.1 | -6.7 | -45.4 |

Regarding the variation of air speed ($u_X$, $u_Y$, $u_Z$, m s$^{-1}$) with the measurement distance to the sprayer ($D$, m), at 1.5 m height in $X=0$, it was determined that they were related by a negative exponential function. Therefore, to perform the MLR analysis data were natural-log-transformed, after having added 1.5 units to each datum to avoid the presence of 0 and negative numbers in the dataset. The results of the analysis showed that the relationship between all the components of the velocity vector and the distance

801    depended on the blades pitch, the channel A width and the sprayer side, and moreover, it

802    was found a quadratic effect with the distance (Table 7, Table 8 and Table 9).

803    **Table 7.** MLR results: regression coefficients for $\ln(u_X + 1.5)$ as a function of $D$ (m),

804    blades pitch, channel A width and sprayer side, at 1.5 m height in $X=0$ ($R^2 = 0.631$).

| Parameter | Estimate | Standard Error | P |
|---|---|---|---|
| Constant | 1.640 | 0.033 | <0.0001 |
| $D$ | -0.303 | 0.015 | <0.0001 |
| $D^2$ | 0.019 | 0.001 | <0.0001 |
| $I_{RIGHT}$ [*] | 0.527 | 0.038 | <0.0001 |
| $I_{WIDTH\_110}$ [**] | -0.244 | 0.038 | <0.0001 |
| $I_{PITCH\_25}$ [***] | 0.062 | 0.014 | <0.0001 |
| $D \times I_{RIGHT}$ | -0.141 | 0.018 | <0.0001 |
| $D \times I_{WIDTH\_110}$ | -0.059 | 0.018 | 0.0008 |
| $D^2 \times I_{RIGHT}$ | 0.006 | 0.001 | 0.0001 |
| $D^2 \times I_{WIDTH\_110}$ | 0.008 | 0.001 | <0.0001 |

[*] $I_{RIGHT} = 1$ for data from the right side of the sprayer, 0 otherwise.
[**] $I_{WIDTH\_110} = 1$ for data obtained with channel A width of 110 mm, 0 otherwise.
[***] $I_{PITCH\_25} = 1$ for data obtained with blades pitch of 25°, 0 otherwise.

805

806    **Table 8.** MLR results: regression coefficients for $\ln(u_Y + 1.5)$ as a function of $D$ (m),

807    blades pitch, channel A width and sprayer side, at 1.5 m height in $X=0$ ($R^2 = 0.835$).

| Parameter | Estimate | Standard Error | P |
|---|---|---|---|
| Constant | 2.419 | 0.025 | <0.0001 |
| $D$ | -0.341 | 0.011 | <0.0001 |
| $D^2$ | 0.015 | 0.001 | <0.0001 |
| $I_{RIGHT}$ [*] | 0.030 | 0.010 | 0.0027 |
| $I_{WIDTH\_110}$ [**] | 0.107 | 0.030 | 0.0003 |
| $I_{PITCH\_30}$ [***] | 0.128 | 0.012 | <0.0001 |
| $I_{PITCH\_25}$ [****] | 0.091 | 0.032 | 0.0048 |
| $D \times I_{WIDTH\_110}$ | -0.164 | 0.014 | <0.0001 |
| $D \times I_{PITCH\_25}$ | 0.038 | 0.015 | 0.0097 |
| $D^2 \times I_{WIDTH\_110}$ | 0.014 | 0.001 | <0.0001 |
| $D^2 \times I_{PITCH\_25}$ | -0.004 | 0.001 | 0.0007 |

[*] $I_{RIGHT} = 1$ for data from the right side of the sprayer, 0 otherwise.
[**] $I_{WIDTH\_110} = 1$ for data obtained with channel A width of 110 mm, 0 otherwise.
[***] $I_{PITCH\_30} = 1$ for data obtained with blades pitch of 30°, 0 otherwise.
[****] $I_{PITCH\_25} = 1$ for data obtained with blades pitch of 25°, 0 otherwise.

808

809    **Table 9.** MLR results: regression coefficients for $\ln(u_Z + 1.5)$ as a function of $D$ (m),

810    blades pitch, channel A width and sprayer side, at 1.5 m height in $X=0$ ($R^2 = 0.802$).

| Parameter | Estimate | Standard Error | P |
|---|---|---|---|
| Constant | 1.554 | 0.021 | <0.0001 |
| $D$ | -0.334 | 0.009 | <0.0001 |
| $D^2$ | 0.022 | 0.001 | <0.0001 |
| $I_{RIGHT}$ [*] | 0.413 | 0.024 | <0.0001 |
| $I_{PITCH\_30}$ [**] | 0.150 | 0.027 | <0.0001 |
| $I_{PITCH\_25}$ [***] | 0.058 | 0.017 | 0.0006 |
| $D \times I_{RIGHT}$ | -0.137 | 0.011 | <0.0001 |
| $D \times I_{WIDTH\_110}$ [****] | -0.041 | 0.005 | <0.0001 |
| $D \times I_{PITCH\_30}$ | -0.045 | 0.012 | 0.0001 |
| $D \times I_{PITCH\_25}$ | -0.008 | 0.003 | 0.0061 |
| $D^2 \times I_{RIGHT}$ | 0.010 | 0.001 | <0.0001 |
| $D^2 \times I_{WIDTH\_110}$ | 0.004 | 0.001 | <0.0001 |
| $D^2 \times I_{PITCH\_30}$ | 0.003 | 0.001 | 0.0027 |

[*] $I_{RIGHT} = 1$ for data from the right side of the sprayer, 0 otherwise.
[**] $I_{PITCH\_30} = 1$ for data obtained with blades pitch of 30°, 0 otherwise.
[***] $I_{PITCH\_25} = 1$ for data obtained with blades pitch of 25°, 0 otherwise.
[****] $I_{WIDTH\_110} = 1$ for data obtained with channel A width of 110 mm, 0 otherwise.

811

812 The resulting model was expressed as a set of equations which have the following
813 expression (Eq. (19)).

814 $$ = \quad \times \quad ^{\times} \quad ^{\times} \quad - 1.5 \tag{19}$$

815 The coefficients $a$, $b$ and $c$ of the Eq. (19) for each particular case were calculated from
816 the coefficients obtained in the MLR analysis (Table 10, Table 11 and Table 12).

817 **Table 10.** Coefficients of the equations (Eq. (19)) for the variation of $u_X$ (m s$^{-1}$) with $D$
818 (m) for each blades pitch, channel A width and sprayer side, at 1.5 m height in $X=0$.

| Channel A width (mm) | Blades pitch (°) | SPRAYER RIGHT SIDE | | | SPRAYER LEFT SIDE | | |
|---|---|---|---|---|---|---|---|
| | | $a$ | $b$ | $c$ | $a$ | $b$ | $c$ |
| 110 | 20 | 6.840 | -0.503 | 0.033 | 4.036 | -0.362 | 0.028 |
| | 25 | 7.279 | -0.503 | 0.033 | 4.295 | -0.362 | 0.028 |
| | 30 | 6.840 | -0.503 | 0.033 | 4.036 | -0.362 | 0.028 |
| 150 | 20 | 8.734 | -0.445 | 0.025 | 5.154 | -0.303 | 0.019 |
| | 25 | 9.294 | -0.445 | 0.025 | 5.484 | -0.303 | 0.019 |
| | 30 | 8.734 | -0.445 | 0.025 | 5.154 | -0.303 | 0.019 |

819

820 **Table 11.** Coefficients of the equations for the variation of $u_Y$ (m s$^{-1}$) with $D$ (m) for
821 each blades pitch, channel A width and sprayer side, at 1.5 m height in $X=0$.

| Channel A width (mm) | Blades pitch (°) | SPRAYER RIGHT SIDE | | | SPRAYER LEFT SIDE | | |
|---|---|---|---|---|---|---|---|
| | | $a$ | $b$ | $c$ | $a$ | $b$ | $c$ |
| 110 | 20 | 12.892 | -0.505 | 0.030 | 12.507 | -0.505 | 0.030 |

| | 25 | 14.114 | -0.468 | 0.025 | 13.693 | -0.468 | 0.025 |
| | 30 | 14.650 | -0.505 | 0.030 | 14.212 | -0.505 | 0.030 |
| 150 | 20 | 11.581 | -0.341 | 0.015 | 11.236 | -0.341 | 0.015 |
| | 25 | 12.680 | -0.304 | 0.011 | 12.301 | -0.304 | 0.011 |
| | 30 | 13.161 | -0.341 | 0.015 | 12.768 | -0.341 | 0.015 |

**Table 12.** Coefficients of the equations for the variation of $u_Z$ (m s$^{-1}$) with $D$ (m) for each blades pitch, channel A width and sprayer side, at 1.5 m height in $X=0$.

| Channel A width (mm) | Blades pitch (°) | SPRAYER RIGHT SIDE | | | SPRAYER LEFT SIDE | | |
|---|---|---|---|---|---|---|---|
| | | *a* | *b* | *c* | *a* | *b* | *c* |
| 110 | 20 | 7.153 | -0.511 | 0.036 | 4.731 | -0.374 | 0.026 |
| | 25 | 7.583 | -0.519 | 0.036 | 4.716 | -0.382 | 0.026 |
| | 30 | 8.309 | -0.556 | 0.038 | 5.495 | -0.419 | 0.029 |
| 150 | 20 | 7.153 | -0.471 | 0.032 | 4.731 | -0.334 | 0.022 |
| | 25 | 7.583 | -0.479 | 0.032 | 5.016 | -0.342 | 0.022 |
| | 30 | 8.309 | -0.515 | 0.035 | 5.495 | -0.378 | 0.025 |

In order to obtain useful information from equations on how configure the sprayer fan, it is important to highight that at 1.5 m height in $X=0$, differences between the sides of the sprayer in the relationship between the air speed and the distance were found, mainly in the $u_X$ and $u_Z$ components, where air speed was generally higher in the right side than in the left side. However, this is something that might only be managed by changing the design of the fan, nor the blades pitch, neither the channel A width. Therefore, the average values between the data of the right and left sides were plotted to help for the configuration of the sprayer to adjust it to the characteristics of canopy and orchard (row spacing, canopy height, canopy half-height diameter, etc.) (Figure 12).

Regarding the $u_X$ component, no differences were found between blades pitch of 20° and 30°, which obtained always higher air speed than 25° (Figure 12a). This component was higher with channel A width of 150 mm close to the sprayer, but this difference dissapeared at 10 m distance. With channel A width of 110 mm, at 5.0 m from the sprayer, air speed had negative values with all blades pitches, which means that the air current was towards the rear part of the sprayer, maybe affected by the suction of the fan. The $u_Y$ component (Figure 12b) was higher than the other two components at all distances. In this component, for all blades pitches, channel A width of 150 mm gave higher air speeds than 110 mm, with higher differences at 3.0 and 5.0 m away from the sprayer. Blades pitch of 20° gave lower speed than the other two tested pitches in all the

845   distances. Blades pitches of 25° and 30° gave the same air speed close to the sprayer,
846   25° gave higher speed at 3.0 and 5.0 m away, while 30° gave higher speed at 10.0 m
847   distance, mainly with the channel A width of 110 mm. Regarding the $u_Z$ component
848   (Figure 12c), channel A width of 150 mm gave higher values. Channel A width of 110
849   mm gave negative values at distances higher than 5.0 m, which means that the current is
850   directed towards the ground. At 1.0 and 3.0 m distance from the sprayer, 30° gave
851   higher air speed than the other two tested blades pitches, but these differences were
852   reduced farther from the sprayer.



853
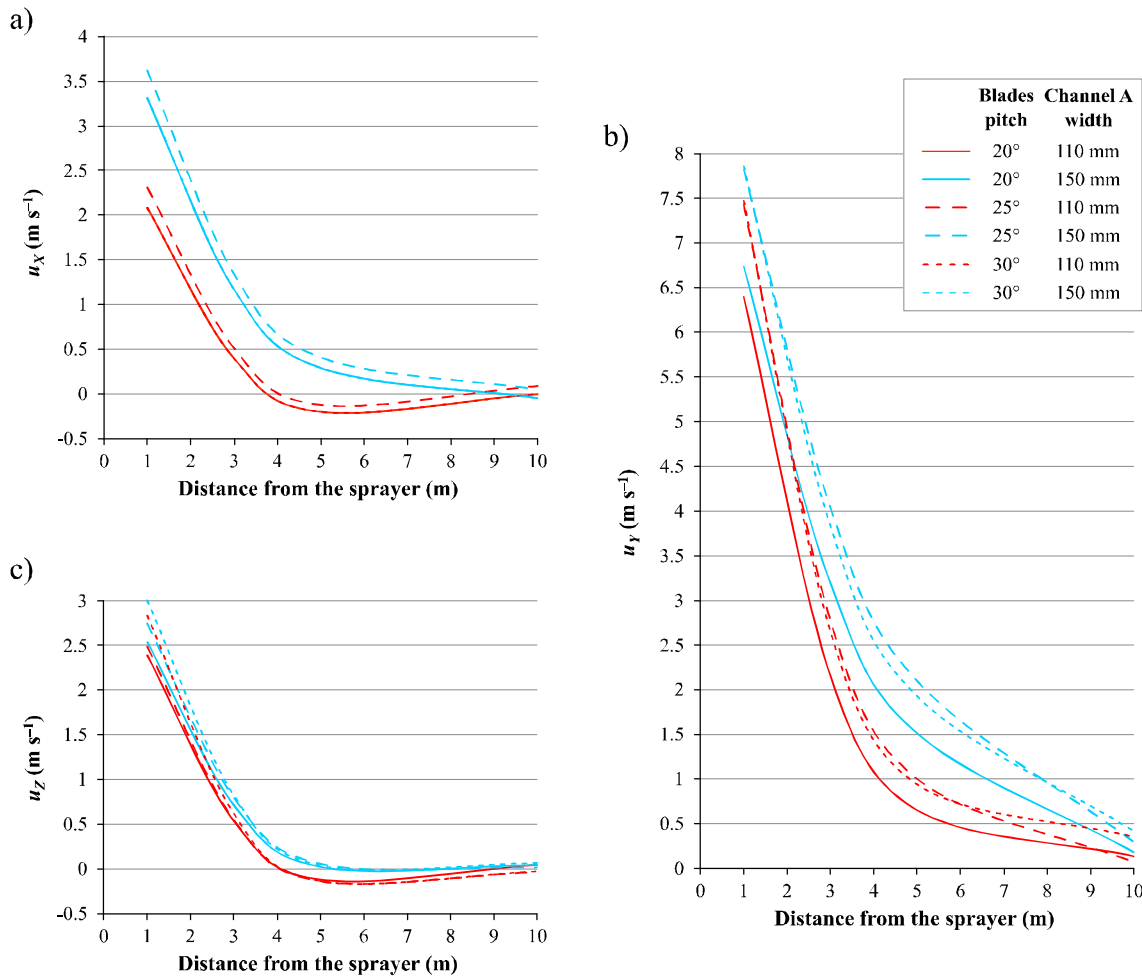
854   **Figure 12.** Mean variation of $u_X$ (a), $u_Y$ (b) and $u_Z$ (c) (m s$^{-1}$) with $D$ (m) for each blades pitch
855   (20°, 25° and 30°) and channel A width (110 and 150 mm), at 1.5 m height in *X=0*.

856

857   The behavior of the air of the equipment was studied in static mode and without
858   considering crop interaction because it is the first step to understand the phenomenon

859 (Delele et al., 2005; García Ramos et al., 2012). From the static characterization of the

860 air flow pattern the fan performance in dynamic conditions, with the sprayer in motion,

861 could be predicted. In fact, some studies have shown the relation between static and

862 dynamic measurements. Increasing the forward speed, the deflexion of the air jet was

863 more pronounced, the width of air jet was narrower and it reached lower distance to the

864 sprayer because the airflow was subjected to the perpendicular action of the forward

865 speed (Reichard et al., 1979; De Moor et al., 2002; Delele et al., 2005; Herrera-Prat et

866 al., 2017). Furthermore, the air velocity decayed faster when the forward speed

867 increased (De Moor et al., 2002; Delele et al., 2005; García-Ramos et al., 2012; Triloff,

868 2011). This is important because it could influence the droplets track, and therefore the

869 pesticide deposition on the leaves. Therefore, knowledge in static conditions will be

870 useful in field application with the aim of regulating the airflow rate and air velocity in

871 relation to the characteristics of the crop and also for understanding the behavior of

872 spray drift.

873 Nevertheless, it would be interesting to characterize the air velocity vectors when the

874 sprayer is moving at the specific range of forward speeds used in high density crops like

875 citrus, because it uses to be in very low range, between 1-3 km h$^{-1}$, and the effect of

876 machine in motion is expected to be lower in comparison with the results obtained by

877 Reichard et al. (1979) who tested at 3.7, 5 and 8 km h$^{-1}$, by De Moor et al. (2002) and

878 Delele et al. (2005) who tested at 0, 6 and 10 km h$^{-1}$ forward speed, by Triloff (2011)

879 who tested at 6, 9 and 12 km h$^{-1}$ forward speed, and by Herrera-Prat et al. (2017) who

880 tested at 0, 2.18, 4.5 and 6.35 km h$^{-1}$. Therefore, future works would be devoted to

881 characterize air velocity vectors in dynamic conditions at low forward speeds with

882 different fan configurations to check the air resistance to the movement of the sprayer,

883 in order to continue delving into the risks of spray drift, and to assess the optimal

884 forward speed, together with the apropriate fan settings, in which the efficiency of the

885 treatments would be maximized.

886

887 *3.4. Turbulence intensity of the airflow in the planes ZY*

888 The turbulence intensity was different depending on the plane and the distance to the

889 equipment (Table 13). At 1.0 m from the fan, the plane *ZY* at *X = 0* m was the most

890     stable, presenting the lowest average intensity values. It is in these circumstances when

891     the air velocities were so high that the fluctuations that occurred had an influence lower

892     than 10% over the magnitude of the air velocity. In the other two planes, as the

893     magnitude was smaller, the fluctuations formed were more considerable over the

894     magnitude. At 3.0 m distance, the lowest turbulent intensity was recorded in the plane *X*

895     *= -0.30 m*. The air current was moving towards that position with respect to *X = 0 m*, as

896     was observed in Fig. 9, Fig. 10 and Fig. 11, and in this section, velocities generated

897     were larger than the fluctuations occurred in the same instant. At the distances of 5.0

898     and 10.0 m from the fan, the turbulence intensities presented a similar character, with

899     values above 30% in most cases. This denoted the more turbulent character of the air

900     stream, although the intensities were higher for the 110 mm than for the 150 mm

901     Channel A width. The magnitudes were lower with this outlet section and, therefore,

902     more sensitive to instantaneous velocity changes (Eq. (17)). However, the proper level

903     of turbulence intensity during pesticide applications with airblast sprayers is a point that

904     has not been thoroughly studied yet. Theoretically, the air turbulence favours the

905     mixture of droplets with the air, moves leaves and branches of the canopies and helps to

906     homogenize the treatment. However, an excessive turbulence may cause unwanted

907     scattering of the sprayed droplets. Future works should check out if the levels of

908     turbulence intensity determined in this trial can help to carry out a more effective

909     treatment.

910

911     **Table 13.** Mean turbulence intensity (*I*, %) from 1.0 to 10.0 m from the fan for each

912     width of Channel A (110 and 150 mm) and fan blades pitch (20°, 25° and 30°).

| Channel A width (mm) | Blades pitch (°) | Plane X (m) | Sprayer side | Distance to the fan (m) | | | |
|---|---|---|---|---|---|---|---|
| | | | | 1.0 | 3.0 | 5.0 | 10.0 |
| | | | | I (%) | I (%) | I (%) | I (%) |
| 110 | 20 | - 0.30 | Left | 25.5 | 12.9 | 37.7 | 41.7 |
| | | | Right | 20.5 | 13.5 | 32.7 | 31.9 |
| | | 0 | Left | 8.8 | 26.0 | 43.0 | 44.8 |
| | | | Right | 8.9 | 28.1 | 42.0 | 32.7 |
| | | + 0.30 | Left | 19.5 | 40.2 | 44.3 | 42.5 |
| | | | Right | 21.4 | 41.3 | 44.7 | 31.4 |
| | 25 | - 0.30 | Left | 19.2 | 12.6 | 37.9 | 42.6 |
| | | | Right | 17.9 | 13.1 | 33.8 | 31.6 |
| | | 0 | Left | 8.9 | 23.4 | 41.1 | 43.4 |
| | | | Right | 9.1 | 28.0 | 40.4 | 30.6 |
| | | + 0.30 | Left | 20.0 | 41.4 | 46.0 | 39.5 |
| | | | Right | 18.7 | 41.8 | 40.9 | 31.2 |
| | 30 | - 0.30 | Left | 19.3 | 11.7 | 35.6 | 42.2 |
| | | | Right | 16.7 | 11.8 | 37.4 | 29.2 |
| | | 0 | Left | 8.4 | 20.2 | 43.6 | 43.0 |
| | | | Right | 9.5 | 29.3 | 42.0 | 30.2 |
| | | + 0.30 | Left | 21.0 | 40.2 | 42.9 | 40.5 |
| | | | Right | 18.9 | 38.6 | 40.9 | 31.9 |
| 150 | 20 | - 0.30 | Left | 35.1 | 21.2 | 34.2 | 35.5 |
| | | | Right | 21.3 | 13.9 | 24.4 | 34.4 |
| | | 0 | Left | 8.5 | 16.7 | 36.1 | 36.3 |
| | | | Right | 8.2 | 16.1 | 31.8 | 35.8 |
| | | + 0.30 | Left | 24.8 | 25.0 | 41.5 | 31.4 |
| | | | Right | 21.1 | 38.8 | 40.6 | 40.3 |
| | 25 | - 0.30 | Left | 27.6 | 20.9 | 29.7 | 36.6 |
| | | | Right | 20.5 | 11.7 | 25.0 | 33.6 |
| | | 0 | Left | 8.7 | 14.2 | 29.9 | 30.5 |
| | | | Right | 9.3 | 15.4 | 32.9 | 40.0 |
| | | + 0.30 | Left | 22.6 | 23.3 | 35.5 | 33.8 |
| | | | Right | 21.4 | 36.6 | 46.6 | 42.8 |
| | 30 | - 0.30 | Left | 28.6 | 19.1 | 30.9 | 37.2 |
| | | | Right | 20.4 | 11.9 | 20.4 | 36.4 |
| | | 0 | Left | 8.9 | 12.6 | 29.3 | 37.0 |
| | | | Right | 9.1 | 12.1 | 25.8 | 37.3 |
| | | + 0.30 | Left | 22.1 | 18.8 | 35.2 | 32.3 |
| | | | Right | 14.5 | 32.6 | 41.0 | 41.5 |

913

914

915 **4. Conclusions**

916 The possibility of having an air regulation system in an airblast sprayer, based on the

917 control of the outlet section and the fan blade pitch, allows the farmers to adjust the

918 outgoing current of the fan to their needs for spray applications based on two

919 variables: the amount of air that comes out (airflow rate) and the velocity with which

920 it moves out. The smaller the outlet section, the lower the outlet airflow rate but the

921 higher the initial velocity. For a same outlet section, an increase in the blade pitch

922 implies an increment in both airflow rate and velocity.

923 In the *ZY* planes, perpendicular to the sprayer and containing the largest air velocity

924 vectors, a width of 110 mm in the adjustable outlet channel (Channel A), generated

925 an air current opening mainly between the plane *X = 0 m* and the plane *X = -0.30 m*,

926 opposite to the advance direction of the tractor. Meanwhile, a width of 150 mm

927 produced a more distributed current between *X = -0.30 m* and *X = +0.30 m*

928 (following the advance direction of the tractor). In both cases, as expected the largest

929 velocity vectors were recorded at *X = 0 m*. These results were strengthen by data

930 collected in the *ZX* planes, parallel to the sprayer. The air presence could be

931 attenuated or magnified increasing or decreasing the blade pitch, respectively.

932 Also the air asymmetry between sprayer sides were affected by the outlet section

933 width and the blade pitch. Considering the plane *X = 0 m* as a reference, for the same

934 blade pitch, the differences in the magnitudes of the vectors between the left and

935 right side were greater with a width of 150 mm than with 110 mm in Channel A,

936 although these variations decreased as the distance to the sprayer increased.

937 Similarly, also the increment of blade pitch produces and increament of air

938 asymmetry.

939 About the general character of the magnitude velocity vectors, for a same blade pitch

940 it was observed that the vectors had greater magnitude at 10.0 m from the sprayer

941 with a width of 150 mm than 110 mm in Channel A, while the differences between

942 magnitudes within the first 5.0 m among consecutive distances were smaller with a

943 width of 150 mm than with 110 mm in Channel A. The lowest turbulence intensity of

944 the air was obtained surroinding the outlet section of the sprayer. In fact, the values

44

945    in the center plane $X = 0\ m$ were very similar to each other up to 1.0 m (8.0 - 9.5 %),

946    regardless of the fan setting. But, from 3.0 m far away the air stream started getting

947    more turbulent in the same plane with 110 mm Channel A wide than 150 mm.

948    The equation that relates the variation of air speed ($u_X$, $u_Y$, $u_Z$, m s$^{-1}$) with the

949    measurement distance to the sprayer considering the significant factors, obtained in

950    this work, will be useful to help the operators and technicians how configure the

951    sprayer fan according the caracteristics of the vegetation in the orchard in order to

952    increase the deposition and reduce the pesticide losses.

953    Once the behavior of the air of the equipment has been characterized and analized in

954    static mode, it would be important to know the behavior in the dynamic mode.

955    Furthermore, it would be necessary to continue studying thorougly what

956    repercussions this would have during a pesticide treatment with this sprayer and how

957    the degree of turbulence easiers the homogeneity of the treatment through field trials.

958

959    **5.  Declarations**

963    **Conflict of interest/Competing interests:** the authors declare that they have no known
964    competing financial interests or personal relationships that could have appeared to
965    influence the work reported in this paper.

966

967    **6.  References**

968    Bahlol, H.Y., Chandel, A.K., Hoheisel, G.A., Khot, L.R., 2019. Smart spray analytical
969           system for orchard sprayer calibration: a-proof-of-concept and preliminary
970           results.      Transactions      of      ASABE,      63(1),      29-35.
971           https://doi.org/10.13031/trans.13196

972    Bahlol, H.Y., Chandel, A.K., Hoheisel, G.-A., Khot, L.R., 2020. The smart spray
973           analytical system: Developing understanding of output air-assist and spray
974           patterns    from    orchard    sprayers.    Crop    Protection,    127,    104977.
975           https://doi.org/10.1016/j.cropro.2019.104977

976    Balsari, P., Grella, M., Marucco, P., Matta, F., Miranda-Fuentes, A., 2019. Assessing the
977           influence of air speed and liquid flow rate on the droplet size and homogeneity
978           in    pneumatic    spraying.    Pest    Management    Science,    75(2),    366-379.
979           https://doi.org/10.1002/ps.5120

980    Balsari, P., Marucco, P., Oggero, G., Tamagnone, M., 2008. Study of optimal air
981           velocities for pesticide application in vineyard. Aspects of Applied Biology, 84,
982           417-424.

983    Berger, L. T., Ortega. P., Gil. E., 2019. Smartomizer ó proactivity and traceability in
984           orchard spraying. In:15th Workshop on Spray Application Techniques in Fruit
985           Growing (Suprofruit), Malling, 16-18 July.

986    Butler-Ellis, M.C.B., Van de Zande, J.C., Van de Berg, F., Kennedy, M.C., O'sullivan,

987      C.M., Jacobs, C.M., Fragkoulis, G., Spanoghe, P., Gerritsen, R., Frewer, L.j.,
988      Charistou, A., 2017. The BROWSE model for predicting exposures of residents
989      and bystanders to agricultural use of plant protection products: an overview.
990      Biosystem           Engineering,          154,          92-104.
991      https://doi.org/10.1016/j.biosystemseng.2016.08.017

992  Cross, J.V., Walklate, P.J., Murray, R.A., Richardson, G.M., 2003. Spray deposits and
993      losses in different sized apple trees from an axial fan orchard sprayer: 3. Effects
994      of    air    volumetric    flow    rate.    Crop    Protection,    22,    381ó394.
995      https://doi.org/10.1016/S0261-2194(02)00192-8

996  Da Silva, A., Sinfort, C., Tinet, C., Pierrat, D., Huberson, S., 2006. A Lagrangian model
997      for spray behavior within vine canopies. Journal of Aerosol Sciencies, 37, 658-
998      674. https://doi.org/10.1016/j.jaerosci.2005.05.016

999  De Moor, A., Langenakens, J., Jaeken, P., 2002. Dynamic air velocity measurements of
1000      air-assisted sprayers in relation to static measurements. Aspects of Applied
1001      Biology, 66, 309-322.

1002  Dekeyser, D., Duga, A.T., Verboven, P., Endalew, A.M., Hendrickx, N., Nuyttens, D.,
1003      2013. Assessment of orchard sprayers using laboratory experiments and
1004      computational fluid dynamics modelling. Biosystem Engineering, 114(2), 157-
1005      169. https://doi.org/10.1016/j.biosystemseng.2012.11.013

1006  Dekeyser, D., Foqué, D., Duga, A.T., Verboven, P., Hendrickx, N., Nuyttens, D., 2014.
1007      Spray deposition assessment using different application techniques in artificial
1008      orchard      trees.      Crop      Protection,      64,      187-197.
1009      https://doi.org/10.1016/j.cropro.2014.06.008

1010  Dekeyser, D., Goossens, T., Melese Endalew, A., Verboven, P., Hendrickx, N., Nuyttens,
1011      D., 2011. Performance assessment of orchard sprayers, Part 1: Machine
1012      Characterization. In: 11th Workshop on Spray Application Techniques in Fruit
1013      Growing (Suprofruit), Bergerac, 8-10 June.

1014  Delele, M.A., De Moor, A., Sonck, B., Ramon, H., Nicolaï, B.M., Verboven, P., 2005.
1015      Modelling and validation of the air flow generated by a cross flow air sprayer as
1016      affected by travel speed and fan speed. Biosystem Engineering, 92, 165-174.

1017          https://doi.org/10.1016/j.biosystemseng.2005.05.018

1018 Delele, M.A., Jaeken, P., Debaer, C., Baetens, K., Endalew, A.M., Ramon, H., 2007.
1019          CFD prototyping of an air-assisted orchard sprayer aimed at drift reduction.
1020          Computers and Electronics in Agriculture, 55(1), 16-27.
1021          https://doi.org/10.1016/j.compag.2006.11.002

1022 Di Prinzio, A., Behmer, S., Magdalena, J., Striebeck, G., 2004. Evaluación comparativa
1023          de dos técnicas de aplicación de agroquímicos en manzanos de alta densidad.
1024          Agro-Ciencia, 20(2), 73-83.

1025 Doruchowski, G., Balsari, P., Gil, E., Marucco, P., Roettele, M., Wehmann, H.-J., 2014.
1026          Environmentally Optimised Sprayer (EOS)-A software application for
1027          comprehensive assessment of environmental safety features of sprayers. Science
1028          of the Total Environment, 482-483, 201-207.
1029          https://doi.org/10.1016/j.scitotenv.2014.02.112

1030 Doruchowski, G., Roettele, M., Herbst, A., Balsari, P., 2013. Drift evaluation tool to
1031          raise awareness and support training on the sustainable use of pesticides by drift
1032          mitigation. Computers and Electronics in Agriculture, 97, 27-34.
1033          https://doi.org/10.1016/j.compag.2013.06.006

1034 Doruchowski, G., Swiechowski, W., Godyn, A., Holownicki, R., 2011. Automatically
1035          controlled sprayer to implement spray drift reducing application strategies in
1036          orchards. Journal of Fruit and Ornamental Plant Research, 19, 175-182.

1037 Endalew, A.M., Debaer, C., Rutten, N., Vercammen, J., Delele, M.A., Ramon, H.,
1038          Nicolaï, B.M., Verboven, P., 2010a. Modeling pesticide flow and deposition
1039          from air-assisted orchard spraying in orchards: A new integrated CFD approach.
1040          Agricultural and Forest Meteorology, 150, 1383-1392.
1041          https://doi.org/10.1016/j.agrformet.2010.07.001

1042 Endalew, A.M., Debaer, C., Rutten, N., Vercammen, J., Delele, M.A., Ramon, H.,
1043          Nicolaï, B.M., Verboven, P., 2010b. A new integrated CFD modelling approach
1044          towards air assisted orchard spraying. Part II. Validation for different sprayer
1045          types. Computers and Electronics in Agriculture, 71(2), 137-147.
1046          https://doi.org/10.1016/j.compag.2009.11.005

1047 Failla, S., Romano, E., Longo, D., Bisaglia, C., Schillaci, G., 2020a. Effect of Different
1048     Axial Fans Configurations on Airflow Rate. In: Innovative Biosystems
1049     Engineering for Sustainable Agriculture, Forestry and Food Production. MID-
1050     TERM AIIA 2019. Lecture Notes in Civil Engineering, vol 67. Springer, Cham

1051 Failla, S., Bisaglia, C., Schillaci, G., Longo, D., Romano, E., 2020b. Sprayer axial fan
1052     layout affecting energy consumption and carbon emissions. Resources, 9, 136.
1053     https://doi.org/10.3390/resources9110136

1054 Felsot, A.S., Unsworth, J.B., Linders, J.B.H.J., Roberts, G., 2011. Agrochemical spray
1055     drift; assessment and mitigation-a review. Journal of Environmental Science and
1056     Health, Part B, 46, 1-23. https://doi.org/10.1080/03601234.2010.515161

1057 Fornasiero, D., Mori, N., Tirello, P., Pozzebon, A., Duso, C., Tescari, E., Bradascio, R.,
1058     Otto, S., 2017. Effect of spray drift reduction techniques on pests and predatory
1059     mites in orchards and vineyards. Crop Protection, 98, 283ó292.
1060     https://doi.org/10.1016/j.cropro.2017.04.010

1061 Fox, R.D., Brazee, R.D., Svensson, S.A., Reichard, D.L., 1992. Air jet velocities from a
1062     cross-flow fan sprayer. Transactions of ASAE, 35, 1381-1384.
1063     https://doi.org/10.13031/2013.28744

1064 Garcerá. C. Berger. L.T., Chueca. P., 2018. Efficiency assessment of H3O Smartomizer
1065     in citrus. Aspects of Applied Biology, 137. 93-100.

1066 Garcerá, C., Fonte, A., Moltó, E., Chueca, P., 2017a. Sustainable use of pesticide
1067     applications in citrus: A support tool for volume rate adjustment. International
1068     Journal of Environmental Research and Public Health, 14(7), 715.
1069     https://doi.org/10.3390/ijerph14070715

1070 Garcerá, C., Moltó, E., Chueca, P., 2017b. Spray pesticide applications in Mediterranean
1071     citrus orchards: canopy deposition and off-target losses. Science of the Total
1072     Environment, 599, 1344-1362. https://doi.org/10.1016/j.scitotenv.2017.05.029

1073 García-Ramos, F.J., Vidal, M., Boné, A., 2009. Field evaluation of an air assisted
1074     sprayer equipped with two reversed rotation fans. Applied Engineering in
1075     Agriculture, 25(4), 481-494. https://doi.org/10.13031/2013.27461

1076 García-Ramos, F.J., Vidal, M., Boné, A., Malón, H., Aguirre, J., 2012. Analysis of the

airflow generated by an air-assisted sprayer equipped with two axial fans using a 3D sonic anemometer. Sensors, 12(6), 7598-7613. https://doi.org/10.3390/s120607598

Gil, E., Llop, J., Gallart, M., Valera, M., Llorens, J., 2015. Design and evaluation of a manual device for air flow rate adjustment in spray application in vineyards. In: 13th Workshop on Spray Application in Fruit Growing (Suprofruit), Lindau, 15-18 July.

Gil, E., Llorens, J., Landers, A., Llop, J., Giralt, L., 2011. Field validation of dosaviña, a decision support system to determine the optimal volume rate for pesticide application in vineyards. European Journal of Agronomy, 35(1), 33-46. https://doi.org/10.1016/j.eja.2011.03.005

Gil, Y., Sinfort, C., 2005. Emission of pesticides to the air during sprayer application: a bibliographic review. Atmospheric Environment, 39(28), 5183-5193. https://doi.org/10.1016/j.atmosenv.2005.05.019

Grella, M., Marucco, P., Manzone, M., Gallart, M., Balsari, P.. 2017a. Effect of sprayer settings on spray drift during pesticide application in poplar plantations (Populus spp.). Science of the Total Environment, 578, 427-439. https://doi.org/10.1016/j.scitotenv.2016.10.205

Grella, M., Miranda-Fuentes, A., Marucco, P., Balsari, P., 2020a. Field assessment of a newly-designed pneumatic spout to contain spray drift in vineyards: evaluation of canopy distribution and off-target losses. Pest Management Science, 76, 4173ó4191. https://doi.org/10.1002/ps.5975

Grella, M., Gallart, M., Marucco, P., Balsari, P., Gil, E., 2017b. Ground deposition and airborne spray drift assessment in vineyard and orchard: the influence of environmental variables and sprayer settings. Sustainability, 9(5), 728. https://doi.org/10.3390/su9050728

Grella, M., Marucco, P., Balsari, P., 2019. Toward a new method to classify the airblast sprayers according to their potential drift reduction: comparison of direct and new indirect measurement methods. Pest Management Science, 75, 2219-2235. https://doi.org/10.1002/ps.5354

1107    Grella, M., Marucco, P., Balsari, P., 2020b. Evaluation of Potential Spray Drift
1108          Generated by Different Types of Airblast Sprayers Using an õad hocö Test Bench
1109          Device. In: Innovative Biosystems Engineering for Sustainable Agriculture,
1110          Forestry and Food Production. MID-TERM AIIA 2019. Lecture Notes in Civil
1111          Engineering, vol 67. Springer, Cham.

1112    Gujarati, D.N., 2003. Basic econometrics. McGraw-Hill, New York.

1113    Herrera-Prat, M.I., García de la Figal-Costales, A.E., de las Cuevas-Milán, H., Martins-
1114          Teixeira, M., 2017. The air speed in the fan and the flow in an agricultural
1115          sprayer. Revista Ciencias Técnicas Agropecuarias, 26: 50-56.

1116    Ho wnicki, R., Doruchowski, G.,  wiechowski, W., Gody , A., Konopacki, P.J., 2017.
1117          Variable air assistance system for orchard sprayers; concept, design and
1118          preliminary       testing.    Biosystem     Engineering,     163,    134-149.
1119          https://doi.org/10.1016/j.biosystemseng.2017.09.004

1120    Jong, F.M.W., Snoo, G.R., Van de Zande, J.C., 2008. Estimated nationwide effects of
1121          pesticide spray drift on terrestrial habitats in the Netherlands. Journal of
1122          Environmental        Management,        86(4),        721-730.
1123          https://doi.org/10.1016/j.jenvman.2006.12.031

1124    Kasner, E.J., Fenske, R.A., Hoheisel, G.A., Galvin, K., Blanco, M.N., Seto, E.Y., Yost,
1125          M.G., 2020. Spray drift from three airblast sprayer technologies in a modern
1126          orchard work environment. Annals of Work Exposures and Health, 64(1), 25ó37.
1127          https://doi.org/10.1093/annweh/wxz080

1128    Llorens, J., Gallart, M., Llop, J., Miranda-Fuentes, A., Gil, E., 2016. Difficulties to
1129          apply ISO 22866 requirements for drift measurements. A particular case of
1130          traditional olive tree plantations. Aspects of Applied Biologists, 132, 31-37.

1131    Llorens, J., Gil, E., Llop, J., Escolà, A., 2010. Variable rate dosing in precision
1132          viticulture: use of electronic devices to improve application efficiency. Crop
1133          Protection, 29, 239-248.

1134    Marucco, P., Balsari, P., Grella, M., Pugliese, M., Eberle, D., Gil Moya, E., Llop
1135          Casamada, J., Fountas, S., Mylonas, N., Tsitsigiannis, D., Balafoutis, A., Polder,
1136          G., Nuyttens, D., Dias, L., Douzals, J.P., 2019. OPTIMA EU project: main goal

1137      and first results of inventory of current spray practices in vineyards and
1138      orchards. In: 15th Workshop on Spray Application and Precision Technology in
1139      Fruit Growing (SuproFruit), East Malling, 16-18 July.

1140    Marucco, P., Balsari,P., Caffini, A., Fountas, S., Gioelli, F., Grella, M., Mylonas, N.,
1141      Nuyttens, D., Zwartvaegher, I., 2020. OPTIMA Project: development of a smart
1142      sprayer for vineyards. Aspects of Applied Biology, 144, 77-83.

1143    Miranda-Fuentes, A., Rodríguez, A., Gil, E., Agüera, J., Gil, J.A., 2015. Influence of
1144      liquid volume and airflow rates on spray application quality and homogeneity in
1145      super intensive olive tree canopies. Science of the Total Environment, 537, 250ó
1146      259. https://doi.org/10.1016/j.scitotenv.2015.08.012

1147    Ochoa, V., Maestroni, B., 2018. Pesticides in water, soil, and sediments. In: Integrated
1148      Analytical Approaches for Pesticide Management. Academic Press, Vienna, pp.
1149      133-147.

1150    Otto, S., Lazzaro, L., Finizio, A., Zanin, G., 2009. Estimating ecotoxicological effects of
1151      pesticide drift on nontarget arthropods in field hedgerows. Environmental
1152      Toxicology and Chemistry, 28(4), 853-863. https://doi.org/0.1897/08-260R.1

1153    Otto, S., Loddo, D., Baldoin, C., Zanin, G., 2015. Spray drift reduction techniques for
1154      vineyards in fragmented landscapes. Journal of Enviromental Management, 162,
1155      290-298. https://doi.org/10.1016/j.jenvman.2015.07.060

1156    Pai, N., Salyani, M., Sweeb, R.D., 2009. Regulating airflow of orchard airblast sprayer
1157      based on tree foliage density. Transactions of ASABE, 52(5), 1423-1428.
1158      https://doi.org/10.13031/2013.29122

1159    Pascuzzi, S., Cerruto, E., Manetto, G., 2017. Foliar spray deposition in a õtendoneö
1160      vineyard as affected by airflow rate, volume rate and vegetative development.
1161      Crop Protection, 91, 34-48. https://doi.org/10.1016/j.cropro.2016.09.009

1162    Pergher, G., 2006. The effect of air flow rate and forward speed on spray deposition
1163      from a vineyard sprayer. Rivista di Ingegneria Agraria, 37, 17-23.

1164    Pergher, G., Gubiani, R., Cividino, S. R., Dell'Antonia, D., Lagazio, C., 2013.
1165      Assessment of spray deposition and recycling rate in the vineyard from a new
1166      type of air-assisted tunnel sprayer. Crop Protection, 45, 6-14.

1167　　　　　https://doi.org/10.1016/j.cropro.2012.11.021

1168　Pope, S.B., 2000. Turbulent Flows. Cambridge University Press, Cambridge.

1169　Randall, J.M., 1971. The relationship between air volume and pressure on spray
1170　　　　　distribution in fruit trees. Journal of Agricultural Engineering Research, 16, 1-
1171　　　　　31. https://doi.org/10.1016/S0021-8634(71)80002-1

1172　Rao, S.S. (Ed), 2018. The Finite Element Method in Engineering. Chapter 17 - Basic
1173　　　　　Equations of Fluid Mechanics. 6$^{th}$ edition. Elsevier. Amsterdam.

1174　Reichard, D.L., Fox, R.D., Brazee, R.D., Hall, F.R., 1979. Air velocities delivered by
1175　　　　　orchard air sprayers. Transactions of the ASAE, 22(1), 69-0074.
1176　　　　　https://doi.org/10.13031/2013.34968

1177　Rüegg, J., Schwizer. Th., Viret, O., 2006. Simplified adjustment of the quantities of
1178　　　　　fungicides and insecticides to the tree volume of stone fruit plants in Switzerland
1179　　　　　(in German). Schweizerische Zeitschrift für Obst- und Weinbau, 237-237.

1180　Salcedo, R., Garcerá, C., Granell, R., Moltó, E., Chueca, P., 2015. Description of the
1181　　　　　airflow produced by an air-assisted sprayer during pesticide applications to
1182　　　　　citrus. Spanish Journal of Agricultural Research, 13, 2-8.
1183　　　　　http://dx.doi.org/10.5424/sjar/2015132-6567

1184　Salcedo, R., Pons, P., Llop, J., Zaragoza, T., Campos, J., Ortega, P., Gallart, M., Gil, E.,
1185　　　　　2019. Dynamic evaluation of airflow stream generated by a reverse system of an
1186　　　　　axial fan sprayer using 3D-ultrasonic anemometers. Effect of canopy structure.
1187　　　　　Computers and Electronics in Agriculture, 163, 104851.
1188　　　　　https://doi.org/10.1016/j.compag.2019.06.006

1189　Salyani, M., Miller, D.R., Farooq, M., Sweeb, R.D., 2013. Effects of sprayer operating
1190　　　　　parameters on airborne drift from citrus air-carrier sprayers. Agricultural
1191　　　　　Engineering International: CIGR Journal, 15(1), 27-36.

1192　Sozzi, A., 2011. Estudio del efecto de diferentes caudales de aire sobre la distribución,
1193　　　　　recubrimiento y cantidad de producto depositado con pulverizador
1194　　　　　hidroneumático en cítricos. Ph.D. Thesis. Universitat Politécnica de València,
1195　　　　　Spain. (In Spanish).

1196　Suits, D.B., 1957. Use of dummy variables in regression equations. Journal of the

1197        American Statistical Association, 52, 548ó551.

1198 Svensson, S. A., Fox, R. D., Hansson, P. A., 2002. Forces on apple trees sprayed with a
1199        cross-flow fan air jet. Transactions of ASAE, 45(4), 889-895.
1200        https://doi.org/10.13031/2013.9935

1201 Svensson, S. A., Brazee, R. D., Fox, R. D., Williams, K. A., 2003. Air jet velocities in
1202        and beyond apple trees from a two-fan cross-flow sprayer. Transactions of
1203        ASAE, 46, 611-621. https://doi.org/10.13031/2013.13587

1204 wiechowski, W., Doruchowski, G., Holownicki, R., Godyn, A., 2004. Penetration of
1205        air within the apple tree canopy as affected by the air jet characteristics and
1206        travel velocity of the sprayer. Electronic Journal of Polish Agricultural
1207        Universities7(2). Available at
1208        http://www.ejpau.media.pl/volume7/issue2/engineering/art-03.html [accessed
1209        April 2020].

1210 TOPPS-Prowadis Project, 2014. Best management practices to reduce spray drift.
1211        Available at http://www.topps-life.org/ [accessed April 2020].

1212 Torrent, X., Garcerá, C., Moltó, E., Chueca, P., Abad, R., Grafulla, C., Román, C.,
1213        Planas, S., 2017. Comparison between standard and drift reducing nozzles for
1214        pesticide application in citrus: Part I. Effects on wind tunnel and field spray drift.
1215        Crop Protection, 96, 130-143.

1216 Triloff, P., 2011. Verlustreduzierter Pflanzenschutz im Baumobstbau.
1217        Abdriftminimierung und Effizienzsteigerung durch baumformabhängige
1218        Dosierung und optimierte Luftführung. Dissertation Universität Hohenheim,
1219        Institut für Agrartechnik, Verlag Grauer, Beuren, Stuttgart, 351.

1220 Triloff, P., 2015. Results of measuring the air distribution of sprayers for 3D-Crops and
1221        parameters for evaluating and comparing fan types. In: 13th Workshop on Spray
1222        Application in Fruit Growing (Suprofruit), Lindau, 15-18 July.

1223 Triloff, P., 2016. Results and conclusions from five years measuring and adjusting air
1224        distribution of brand new sprayers for 3D-Crops. In: 6th european workshop on
1225        standard procedure for the inspection of sprayers in Europe (SPISE),
1226        Castelldefels, 13-15 September.

1227 Van de Zande. J.C., Schlepers. M., Hofstee. J.W., Michielsen. J.G.P., Wenneker. M.,
1228   2017. Characterization of the air flow and the liquid distribution of orchard
1229   sprayers. In: 14th Workshop on Spray Application Techniques in Fruit Growing
1230   (Suprofruit), Hasselt, 10-12 July.

1231 Vereecke, E., Langenakens, J., De Moor, A., Pieters, M., Jaeken, P., 2000. The air
1232   distribution generated by air-assisted orchard sprayers. International Symposium
1233   of Crop Protection, 65, 991ó1000.

1234 Walklate, P.J., Weiner, K.L., Parkin, C.S., 1996. Analysis of and experiment
1235   measurements made on a moving air-assisted sprayer with two-dimensional air-
1236   jets penetrating a uniform crop canopy. Journal of Agricultural Engineering
1237   Research, 63(4), 365ó378. https://doi.org/10.1006/jaer.1996.0039

1238 Wenneker, M., Van de Zande, J.C., Michielsen, J.M.G.P., Stalling, H., Van Dalfsen, P.,
1239   Snoussi, M., De Hoog, D.C., 2020. Spray deposition on apple trees in the early
1240   stages of tree development: effect of sprayer type, nozzle type and air setting.
1241   Aspects of Applied Biology, 144, 43-50.

1242 Whitney, J.D., Hedden, S.L., Churchill, D.B., Cromwell, R.P., 1986. Performance
1243   characteristics of PTO airblast sprayers for citrus. Proceedings of the Florida
1244   State Horticultural Society, 99, 59-65.

1245 Zhu, H., Brazee, R.D., Derksen, R.C., Fox, R.D., Krause, C.R., Ozkan, H.E., Losely, K.,
1246   2006. A specially designed air-assisted sprayer to improve spray penetration and
1247   air jet velocity distribution inside dense nursery crops. Transactions of ASABE,
1248   49(5), 1285-1294. https://doi.org/10.13031/2013.2203

1249